Chapter 6

Modelling of aggregation processes

Nomenclature

a_i	radius of particle i
A	Hamaker constant
B	constant in eqn (6.43)
c	electrolyte concentration
C	constant in eqn (6.47)
d	separation distance between particle surfaces
d_F	fractal dimension
d_{max}	limiting aggregate size
D_i	diffusion coefficient of particle i
D_{ij}	mutual diffusion coefficient for particles i and j
e	electronic charge (1.602×10^{-19} C)
f	fraction of added polymer necessary for destabilization
$f(x)$	frequency function
g	gravitational acceleration
G	shear rate
J_i	flux of i-particles to a sphere
J_{ij}	collision frequency for particles of type i and j
k	Boltzmann's constant (1.381×10^{-23} J K^{-1})
k'	aggregation number
$\bar{k}$	average aggregation number
k_a	aggregation rate constant
k_{ij}	collision rate constant for particles of type i and j
L	size of aggregate
M	mass of aggregate
n	exponent in eqn (6.47)
n_0	initial concentration of primary particles
n_i	number concentration of particles of type i
n_T	total particle concentration
R_{ij}	collision radius for particles i and j
t	time
t_{Ads}	characteristic adsorption time
T	absolute temperature
u	dimensionless separation distance – see eqn (6.32)
v	volume of an aggregate
v_g	number median particle volume
v_T	total volume of particles

w degree of homogeneity – see eqn (6.53)
W stability ratio
x dimensionless aggregate size – see eqn (6.50)
y exponent in eqn (6.43)
z valence of ion

α collision efficiency
α_0 limiting collision efficiency
$\beta(u)$ function of u, given in eqn (6.36)
γ dimensionless function of surface potential – see eqn (6.35)
δ separation of particles in primary minimum (m)
ϵ power input per unit mass
ζ electrokinetic (zeta) potential
η_K Kolmogoroff microscale
θ fractional surface coverage
κ Debye–Hückel parameter
λ wavelength
μ dynamic viscosity
ν kinematic viscosity
ρ density of fluid
ρ_E effective (buoyant) density of aggregate
ρ_s density of particle
σ geometrical standard deviation
τ characteristic aggregation time
ϕ volume fraction
ϕ_A Van der Waals interaction
ϕ_{max} height of energy barrier
ϕ_T total interaction energy
ψ_δ Stern potential

6.1 Collisions and aggregation: the Smoluchowski approach

Most discussions of the rate of aggregation start from the classic work of Smoluchowski (1917), which laid the foundations of the subject. It is convenient to think in terms of a dispersion of initially identical particles (primary particles), which, after a period of aggregation, contains aggregates of various sizes and different concentrations – n_i particles of size i, n_j particles of size j etc. Here, n_i etc. refer to the number concentrations of different aggregates and 'size' implies the number of primary particles comprising the aggregate; we can speak of 'i-fold' and 'j-fold' aggregates. A fundamental assumption is that aggregation is a second-order rate process, in which the rate of collision is proportional to the product of concentrations of two colliding species. (Three-body collisions are usually ignored in treatments of aggregation – they only become important at

very high particle concentrations). Thus, the number of collisions occurring between i and j particles in unit time and unit volume, J_{ij}, is given by:

$$J_{ij} = k_{ij} n_i n_j \tag{6.1}$$

where k_{ij} is a second-order rate constant, which depends on a number of factors, such as particle size and transport mechanism (see below).

In considering the rate of aggregation, we must recognize that, because of interparticle forces, not all collisions may be successful in producing aggregates. The fraction of successful collisions is called the collision efficiency and given the symbol α. If there is strong repulsion between particles then practically no collision gives an aggregate and $\alpha \approx 0$. When there is no significant net repulsion or when there is an attraction between particles, then the collision efficiency can approach unity.

Although there are some theoretical difficulties, it is usual to assume that the collision rate is independent of colloid interactions and depends only on particle transport. This assumption can often be justified on the basis of the short-range nature of interparticle forces, which operate over a range which is usually much less than the particle size, so that particles are nearly in contact before these forces come into play. The 'decoupling' of transport and attachment steps greatly simplifies the analysis of aggregation kinetics and a similar assumption is common in simple treatments of particle deposition.

A very important case where this approach is not justified is that of hydrodynamic or viscous interaction, which involves much longer-range effects. This will be treated separately in Section 6.3.3.

For the present, we shall assume that every collision is effective in forming an aggregate (i.e. the collision efficiency, $\alpha = 1$), so that the aggregation rate constant is the same as the collision rate constant. It is then possible to write the following expression for the rate of change of concentration of k-fold aggregates, where $k = i + j$:

$$\frac{dn_k}{dt} = \frac{1}{2} \sum_{\substack{i+j \to k \\ i=1}}^{i=k-1} k_{ij} n_i n_j - n_k \sum_{k=1}^{\infty} k_{ik} n_i \tag{6.2}$$

The first term on the right-hand side represents the rate of formation of k-fold aggregates by collision of any pair of aggregates, i and j, such that $i + j = k$. Carrying out the summation by this method would mean counting each collision twice and hence the factor 1/2 is included. The second term accounts for the loss of k-fold aggregates by collision, and aggregation, with any other aggregates. The terms k_{ij} and k_{ik} are the appropriate rate constants. It is important to note that eqn (6.2) is for *irreversible* aggregation, since no allowance is made for break-up of aggregates.

For continuous particle size distributions, an integral version of eqn (6.2) can be written. In principle, it is then possible to derive the evolution of the aggregate size distribution with time (see Section 6.6.1), but there are formidable difficulties, especially in assigning values to the rate coefficients. These depend greatly on the nature of the particles and on the way in which collisions are

brought about. The simplest assumption is that spherical particles *coalesce* on contact to form a larger sphere with the same total volume. This is physically unrealistic except for liquid (emulsion) droplets, but has often been assumed in earlier treatments of aggregation kinetics.

There are three important transport mechanisms in practice: (1) Brownian diffusion (giving *perikinetic* aggregation); (2) fluid motion (*orthokinetic* aggregation); and (3) differential settling. These will be considered in the next section. In all cases, we shall assume that the particles are spherical and that the collision efficiency is unity (every collision is effective in forming a permanent aggregate). Also, hydrodynamic interaction will be neglected for the time being. Although these assumptions are not realistic for practical systems, they enable simple results to be derived which can be used to illustrate the essential features of the various aggregation mechanisms.

Effects of colloidal and hydrodynamic interactions on aggregation rates will be considered in Section 6.3.

6.2 Collision mechanisms

6.2.1 Perikinetic aggregation

Small particles in suspension can be seen to undergo continuous random movements or Brownian motion. The diffusion coefficient of a spherical particle is given by the Stokes–Einstein equation:

$$D_i = \frac{kT}{6\pi a_i \mu} \tag{6.3}$$

where k is Boltzmann's constant, T the absolute temperature, a_i the particle radius and μ the viscosity of the suspending fluid.

Smoluchowski (1917) calculated the rate of diffusion of spherical particles of type i to a fixed sphere j. If each i particle is captured by the central sphere on contact, then the i particles are effectively removed from the suspension and a concentration gradient is established in the radial direction towards the sphere, j. After a very brief interval, steady-state conditions are established and it can easily be shown that the number of i particles contacting j in unit time is:

$$J_i = 4\pi R_{ij} D_i n_i \tag{6.4}$$

where D_i is the diffusion coefficient of particles of type i and n_i is their concentration in the bulk suspension. R_{ij} is the collision radius for particles i and j, which is the centre-to-centre distance at which they may be taken to be in contact. In practice, it can usually be assumed that this is simply the sum of the particle radii, i.e:

$$R_{ij} = a_i + a_j \tag{6.5}$$

When there is significant long-range attraction between particles they may be effectively 'captured' at greater distances, so that the collision radius is rather

larger than that given by eqn (6.5). However, there is usually very little error in using this approximation.

Of course, in practice, the central sphere j is not fixed, but is itself subject to Brownian diffusion. It is only necessary to replace D_i in (6.4) by the *mutual diffusion coefficient*, D_{ij}, to account for the motion of the j particle, with:

$$D_{ij} = D_i + D_j \tag{6.6}$$

If the concentration of j particles is n_j, then the number of i–j collisions occurring in unit volume per unit time is simply:

$$J_{ij} = 4\pi R_{ij} D_{ij} n_i n_j \tag{6.7}$$

Comparing this with eqn (6.1) gives the rate constant for perikinetic collisions, which after substituting for R_{ij} and D_{ij}, using eqns (6.3), (6.5) and (6.6), gives:

$$k_{ij} = \frac{2kT}{3\mu} \frac{(a_i + a_j)^2}{a_i a_j} \tag{6.8}$$

This result has the very important feature that, for particles of approximately equal size, the collision rate constant becomes almost independent of particle size. The term $(a_i + a_j)^2/a_i a_j$ has a constant value of about 4 when $a_i \approx a_j$. Physically, this is because increasing particle size leads to a lower diffusion coefficient, but a larger collision radius and these two effects cancel each other out when the particles are of nearly the same size. Under these conditions, the rate constant becomes:

$$k_{ij} = \frac{8kT}{3\mu} \tag{6.9}$$

Inserting values appropriate to aqueous dispersions at 25°C gives $k_{ij} = 1.23 \times 10^{-17}\ \mathrm{m^3 s^{-1}}$.

For particles of different size, eqn (6.8) shows that the collision rate constant will always be *greater* than that for equal particles. However, the assumption of a constant value of k_{ij} is a reasonable approximation for particles which differ in size by a factor of about 2 or less.

We can now return to eqn (6.2) and insert the appropriate values for the rate constants, giving the rate of change of aggregate concentration. The simplest case to consider is the very early stages of the aggregation of a monodisperse suspension. The change in the concentration of *primary* particles, n_1, can be calculated from only the second term on the right-hand side of eqn (6.2) since only the loss of such particles needs to be considered. Furthermore, the loss of primary particles, in the early stages, is almost entirely caused by collisions with other primary particles, since there are very few aggregates. This leads to the result:

$$\left(\frac{\mathrm{d}n_1}{\mathrm{d}t}\right)_{t \to 0} = -k_{11} n_1^2 \tag{6.10}$$

where k_{11} is the rate constant for primary particle collisions and has the value given in eqn (6.9).

The initial rate of decrease of the *total* particle concentration, n_T can also be calculated, since each binary collision leads to the loss of *one* particle (two primary particles lost, one aggregate gained):

$$\left(\frac{dn_T}{dt}\right)_{t\to 0} = -\frac{k_{11}}{2} n_1^2 \tag{6.11}$$

The rate constant in this case, $k_{11}/2$, is sometimes called the *aggregation rate constant* and will here be given the symbol k_a. (In other texts, the same quantity may be called the *coagulation* or *flocculation* rate constant.) The factor ½ applied to k_{11} to give the aggregation rate constant has sometimes been a source of confusion, although there is a clear physical meaning. For aqueous dispersions at 25°, the aggregation rate constant has a value of $6.13 \times 10^{-18}\,m^3s^{-1}$.

These expressions could be integrated to give the concentration of primary particles and the total particle concentration as a function of time, but the restriction to $t\to 0$ would limit the utility of the results. In fact, Smoluchowski showed that this approach is not restricted to the very early stages of the aggregation process. If we use eqn (6.2) to write the rate of change of concentration of the various aggregates as:

$$\begin{aligned}
\frac{dn_1}{dt} &= -k_{11}n_1^2 - k_{12}n_1n_2 - k_{13}n_1n_3 \ldots \\
\frac{dn_2}{dt} &= \tfrac{1}{2}k_{11}n_1^2 - k_{12}n_1n_2 - k_{23}n_2n_3 \ldots \\
\frac{dn_3}{dt} &= \tfrac{1}{2}k_{12}n_1n_2 - k_{13}n_1n_3 - k_{23}n_2n_3 \ldots
\end{aligned} \tag{6.12}$$

then the rate of change of the *total* particle concentration can be obtained by summing the terms in eqn (6.12), provided that all of the rate constants, k_{11}, k_{12}, etc., are assumed to be equal. It was shown above that, for particles not too different in size, this is a reasonable assumption and the collision rate constant is then given by eqn (6.9). This approach leads to the very simple result:

$$\frac{dn_T}{dt} = -k_a n_T^2 \tag{6.13}$$

where $n_T = n_1 + n_2 + n_3 + \ldots$ and $k_a = 4kT/3\mu$, as explained above.

The only difference between eqns (6.11) and (6.13) is that the latter contains n_T on the right-hand side, rather than n_1, which enables eqn (6.13) to be integrated immediately. With the initial condition $n_T = n_0$ when $t = 0$ (n_0 is the initial concentration of primary particles), the result is:

$$n_T = \frac{n_0}{1 + k_a n_0 t} \tag{6.14}$$

It can be seen from eqn (6.14) that the total particle concentration is reduced to half of the initial value after a characteristic aggregation time, τ, given by:

$$\tau = \frac{1}{k_a n_0} \tag{6.15}$$

This characteristic time is sometimes called the *coagulation time* or the *half-life* of the aggregation. It can also be thought of as the average time that a particle in the original suspension spends before colliding with another particle. Since the value of k_a is known for given conditions (e.g. $6.13 \times 10^{-18}\,m^3\,s^{-1}$ in water at 25°C), it is possible to calculate typical values of τ, which then depend only on the initial particle concentration. For an aqueous dispersion with $n_0 = 10^9\,cm^{-3}$ (corresponding to a volume fraction of about 5×10^{-4}, for spherical particles of 1 μm diameter) the characteristic time would be about 163 s. For a 100-fold greater particle concentration (a volume fraction of about 5% for 1-μm particles), τ would be less than 2 s.

With the above definition of τ, eqn (6.14) can be rewritten as:

$$n_T = \frac{n_0}{1 + t/\tau} \tag{6.16}$$

It is worth stressing that this expression is based on the assumptions of constant k_{ij} values and that the colliding particles are spherical. The latter assumption implies that 'coalescence' of particles occurs after collision, which may be reasonable in the case of emulsion droplets, but cannot hold for solid particles, where various aggregate shapes can arise (see Section 6.4.1). However, provided that the decrease in diffusion coefficient is roughly balanced by the increase in collision radius as aggregates grow, then the previous treatment should still be reasonably applicable.

The ratio of the initial particle number to the total number after a period of aggregation, n_0/n_T, is a measure of the average aggregate size (the average number of primary particles in an aggregate) and hence a measure of the mean aggregate *volume*. Equation (6.16) shows that the average volume increases linearly with time, for $t \gg \tau$. For 'coalesced spheres' this means that the aggregate radius should increase linearly with the *cube root* of time.

In many practical applications of aggregation, such as the flocculation process in water treatment, it is required to produce large aggregates, containing thousands of primary particles, implying a very large reduction in total particle number. It follows from eqn (6.16) that a reduction of particle concentration, by a factor of, say, 1000 (giving an average aggregate of 1000 primary particles), would require a time of about 1000τ. For dilute suspensions this could represent many hours or days. Even for concentrated suspensions, several minutes may be needed to achieve a large degree of aggregation. For this reason practical flocculation processes can rarely be carried out relying only on Brownian motion to bring about the required collisions.

It is also possible from eqn (6.12) to derive the concentrations of individual aggregate types at different times:

$$n_1 = \frac{n_0}{(1 + t/\tau)^2}$$

$$n_2 = \frac{n_0(t/\tau)}{(1 + t/\tau)^3} \tag{6.17}$$

$$n_k = \frac{n_0(t/\tau)^{k-1}}{(1 + t/\tau)^{k+1}}$$

Results from these expressions are plotted in Figure 6.1, for aggregates up to trimers, showing the dimensionless aggregate concentration n_k/n_0 against the reduced time t/τ. It is clear that, for all aggregates, the concentration passes through a maximum at a certain time and then declines slowly. At all times the concentration of singlets (primary, unaggregated particles) exceeds that of any other individual aggregate type.

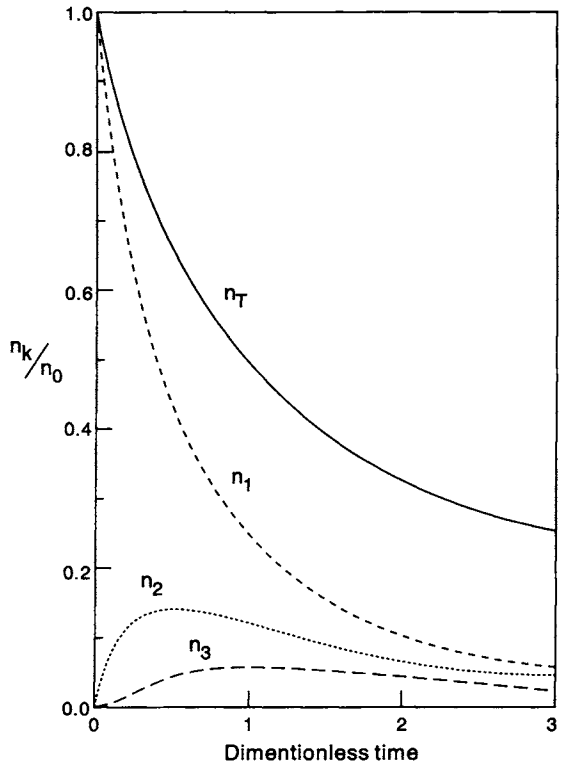

Figure 6.1 *Concentrations of primary particles* (n_1), *doublets* (n_2), *triplets* (n_3) *and total particles* (n_T) *as a function of reduced time* (t/τ), *according to the Smoluchowski result, eqn (6.17). All concentrations are expressed as fractions of the initial concentration of primary particles,* n_0

Despite the simplifying assumptions made in deriving eqn (6.17), it gives reasonable agreement with measured aggregate size distributions in the early stages of the process, although with a value of k_a somewhat lower than that calculated above (Sonntag, 1993). The simple Smoluchowski approach cannot be expected to apply after substantial aggregation has occurred. In such cases, collisions between aggregates of very different sizes become significant, for which the collision rate constant will, according to eqn (6.8), be larger than that assumed here. Also, as aggregates grow, the assumption of spherical shape, implicit in the Smoluchowski treatment, becomes more doubtful. This topic will be deferred for discussion in Section 6.4.

6.2.2 Orthokinetic aggregation

We have seen that collisions brought about by Brownian motion do not generally lead to the rapid formation of very large aggregates, especially in dilute suspensions. In practice, aggregation (flocculation) processes are nearly always carried out under conditions where the suspension is subjected to some form of shear, either by stirring or by flow. Particle transport brought about by fluid motion can give an enormous increase in the rate of interparticle collisions, and aggregation brought about in this way is known as *orthokinetic aggregation*. The first treatment of the rate of orthokinetic aggregation was also due to Smoluchowski (1917), who considered only the case of uniform laminar shear. Such conditions are rarely, if ever, encountered in practice, but it is convenient to start from this simple case and then to modify the result for other conditions.

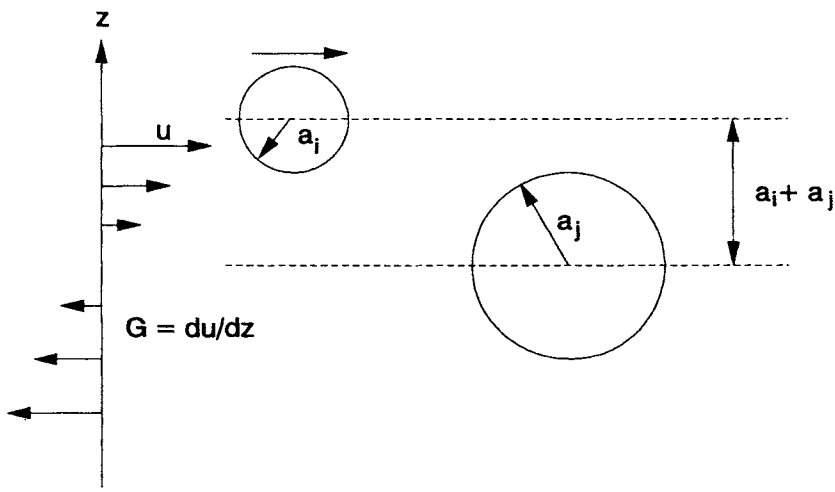

Figure 6.2 *Model for orthokinetic collision of spheres in a uniform shear field. The particles are on streamlines which are separated by a distance equal to the collision radius,* $a_i + a_j$, *and so will just collide*

A uniform laminar shear field is one in which the fluid velocity varies linearly in only one direction, perpendicular to the direction of flow. Smoluchowski assumed that particles would follow straight fluid streamlines and collide with particles moving on different streamlines, according to their relative position. The collision frequency depends on the sizes of the particles and on the velocity gradient or *shear rate*, G. By considering a fixed central sphere of radius a_j and flowing particles of radius a_i, it can be assumed that those moving particles on streamlines that bring their centres within a distance $a_i + a_j$ (the collision radius, R_{ij}) of the central particle will collide with it (Figure 6.2). The collision frequency can then be calculated by considering the flux of particles through a cylinder of radius R_{ij}, the axis of which passes through the centre of the fixed sphere j. For the conditions of Figure 6.2 it is clear that the particles in the upper half of the cylinder will move from left to right and vice versa. The total flux towards the central particle, J_i is just twice that in one half of the cylinder and is given by:

$$J_i = 4Gn_i \int_0^{R_{ij}} z \sqrt{(R_{ij}^2 - z^2)}\ \mathrm{d}z = \frac{4}{3} G n_i R_{ij}^3 \tag{6.18}$$

The total number of collisions occurring between i and j particles in unit volume and unit time is then simply:

$$J_{ij} = \frac{4}{3} n_i n_j G (a_i + a_j)^3 \tag{6.19}$$

It follows, by analogy with eqn (6.1), that the rate constant for orthokinetic collisions between i and j particles is:

$$k_{ij} = \frac{4}{3} G (a_i + a_j)^3 \tag{6.20}$$

The most important difference between this result and the corresponding rate constant for perikinetic collisions, eqn (6.8), is the dependence on the sizes of the colliding particles. As pointed out in Section 6.2.1, for particles of roughly equal size the perikinetic collision rate constant is nearly independent of particle size. This is most definitely not the case for orthokinetic collisions, where the rate is proportional to the *cube* of the collision radius, which has a major effect on aggregate growth rate. As aggregation proceeds and the aggregate size increases, the chance of capture becomes greater. Physically, it is clear that a large particle in a flowing or stirred suspension 'sweeps out' a larger volume than a smaller particle and has a greater opportunity of colliding with other particles. In the perikinetic case, the increased collision radius is largely compensated by the lower diffusion coefficient of larger particles.

The great dependence of the rate constant on particle size means that the assumption of a constant value of k_{ij} is not acceptable beyond the very early stages of aggregation, and aggregate concentrations, as in Figure 6.1, cannot be derived analytically. It is possible, making assumptions about the form of aggregates, to carry out numerical computations of aggregate size distributions under orthokinetic conditions (e.g. Wiesner, 1992), but this subject will be considered in Section 6.5.

For the sake of comparison with the perikinetic case, the rate of reduction in total particle concentration as a result of orthokinetic aggregation can be derived for the initial stages of the process where practically all collisions are between primary particles. By analogy with eqn (6.13), the corresponding orthokinetic rate is:

$$\frac{dn_T}{dt} = -\frac{16}{3} n_T^2 G a_1^3 \tag{6.21}$$

It has been assumed that the rate constant is given by eqn (6.20), with $a_i = a_j = a_1$, the primary particle radius, and that the total particle concentration can be taken as that of primary particles, which will only be the case in the very early stages of aggregation.

Despite its limitations, eqn (6.21) provides a useful comparison with the corresponding perikinetic expression, eqn (6.13). The ratio of the aggregation rate constants is:

$$\frac{k_a(\text{ortho})}{k_a(\text{peri})} = \frac{4G\mu a_1^3}{kT} \tag{6.22}$$

The aggregation rate constants are equal for particles of diameter 1 μm and a shear rate of about $10\,s^{-1}$ (corresponding to only mild agitation), for aqueous dispersions at room temperature. With higher shear rates and (especially) larger particles, the orthokinetic rate becomes very much greater. This explains, at least in a qualitative manner, why stirring of suspensions gives a very great improvement in the aggregation rate.

The form of eqn (6.21) is such that a simple transformation gives the result in terms of the *volume fraction*, ϕ, of the suspended particles ($=4\pi a_1^3 n_T/3$):

$$\frac{dn_T}{dt} = -\frac{4G\phi n_T}{\pi} \tag{6.23}$$

If ϕ is assumed to remain constant during the aggregation process in a closed system, then eqn (6.23) suggests a simple first-order rate law, which can be integrated to give:

$$\frac{n_T}{n_0} = \exp\left(\frac{-4G\phi t}{\pi}\right) \tag{6.24}$$

The particle concentration should thus decrease exponentially with time (and hence the average aggregate size, n_0/n_T, should increase exponentially with time). This type of behaviour has been found experimentally in some cases (Higashitani *et al.*, 1980). Although the assumption of constant volume fraction of the dispersed phase might appear reasonable from the standpoint of mass conservation, this is not the case. Growing aggregates usually adopt a rather open, *fractal* structure (see Section 6.4.1), which means that the effective occupied volume can be much larger than the total volume of the primary particles. The collision radius of an aggregate is greater than that calculated assuming 'coalesced spheres' and leads to more rapid aggregation than that predicted by eqn (6.24) (Jiang and Logan, 1991).

Nevertheless, the simplicity of eqn (6.24) has led to its widespread use for the design of practical flocculation units. At least it points out the importance of shear rate and solids concentration on the flocculation rate. For a fixed solids concentration, the extent of flocculation depends on the dimensionless number Gt, often called the 'Camp number' after Thomas R. Camp (Camp, 1953). In principle, the same degree of aggregation could be achieved by a short period of high shear or a long period of low shear, provided that the value of Gt was maintained constant. By increasing volume fraction, the same relative degree of aggregation (n_0/n_T) can be achieved with a smaller Gt value, a feature which is exploited in many practical flocculation units, where a region of high solids concentration is maintained, e.g. in upflow clarifiers or with solids recirculation. A more satisfactory dimensionless number related to the degree of aggregation is $G\phi t$ (Tambo and Watanabe, 1979), since this includes the particle concentration.

So far, it has been assumed that particles are in a uniform laminar shear field, but this is not a realistic assumption for real flocculation processes, which are carried out under turbulent conditions. One way of approaching this problem (Camp and Stein, 1943) is to calculate a mean velocity gradient, $\overline{G}$, from the power input per unit mass of fluid, ϵ:

$$\overline{G} = \sqrt{\frac{\epsilon}{\nu}} \tag{6.25}$$

where ν is the kinematic viscosity of the fluid ($= \mu/\rho$, where ρ is the density).

This average shear rate can then be inserted, in place of G, in the appropriate Smoluchowski expression, such as eqn (6.19):

$$J_{ij} = \left(\frac{4}{3}\right) n_i n_j \left(\frac{\epsilon}{\nu}\right)^{1/2} (a_i + a_j)^3 \tag{6.26}$$

The result is very like a more rigorous expression derived by Saffman and Turner (1956) for particle collisions in isotropic turbulence, but with a slightly different numerical factor (4/3 rather than 1.29). This apparent agreement is likely to be fortuitous, since the simple averaging procedure in the Camp and Stein approach is not well suited to the highly complex nature of turbulent flow (Spielman, 1978).

Turbulent flow is characterized by eddies of various sizes. The largest eddies are of comparable size to the vessel or impeller. The energy in large-scale eddies cascades through eddies of decreasing size, until, below a certain length scale, the energy is dissipated as heat. The well-known *Kolmogoroff microscale* separates the *inertial range*, where energy is transferred with very little dissipation, from the *viscous subrange*, where the energy is dissipated as heat. This length scale is given by:

$$\eta_K = \left(\frac{\nu^3}{\epsilon}\right)^{1/4} \tag{6.27}$$

For typical values of average shear rate ($\overline{G} \approx 50\text{–}100\,s^{-1}$) in aqueous dispersions, the Kolmogoroff microscale is of the order of 100–150 μm. The

collision rate of particles smaller than η should be reasonably well approximated by an expression of the form of eqn (6.26), although with some uncertainty over the numerical factor. For larger particles, transport by eddies in the inertial range is important and it is likely that the collision rate shows a different dependence on power input – proportional to $\epsilon^{2/3}$ rather than $\epsilon^{1/2}$ (Cleasby, 1984). However, aggregates in this size range (>100 μm) are more likely to be broken in turbulent flow and so it is more difficult to draw conclusions about the rate of floc growth (see Section 6.5).

6.2.3 Differential sedimentation

Another important collision mechanism arises whenever particles of different size or density are settling from a suspension. Larger particles will sediment faster than smaller ones and can capture the latter as they fall. The appropriate rate can be easily calculated, assuming spherical particles and using Stokes' law for their sedimentation rate; see, for example Friedlander (1977). The resulting collision frequency, for particles of equal density, is:

$$J_{ij} = \left(\frac{2\pi g}{9\mu}\right)(\rho_s - \rho) n_i n_j (a_i + a_j)^3 (a_i - a_j) \tag{6.28}$$

where g is the acceleration due to gravity, ρ_s is the density of the particles and ρ is the density of the fluid.

Clearly, differential settling will be more important when the particles are large and dense and in such cases this collision mechanism can be very important in promoting aggregation. Even for an initially uniform suspension of equal particles, aggregates of different size will be formed which settle at different rates. It is often in the later stages of flocculation that floc growth by sedimentation becomes significant.

6.2.4 Comparison of rates

Since we have now covered the most important collision mechanisms, it is convenient to compare the rates for typical conditions. The simplest comparison is between the various collision rate constants, defined by eqn (6.1). These are, for the different mechanisms, repeating previous equations for convenience:

$$\text{Perikinetic: } k_{ij} = \frac{2kT}{3\mu}\frac{(a_i + a_j)^2}{a_i a_j}$$

$$\text{Orthokinetic: } k_{ij} = \frac{4}{3} G(a_i + a_j)^3 \tag{6.29}$$

$$\text{Differential settling: } k_{ij} = \left(\frac{2\pi g}{9\mu}\right)(\rho_s - \rho)(a_i + a_j)^3 (a_i - a_j)$$

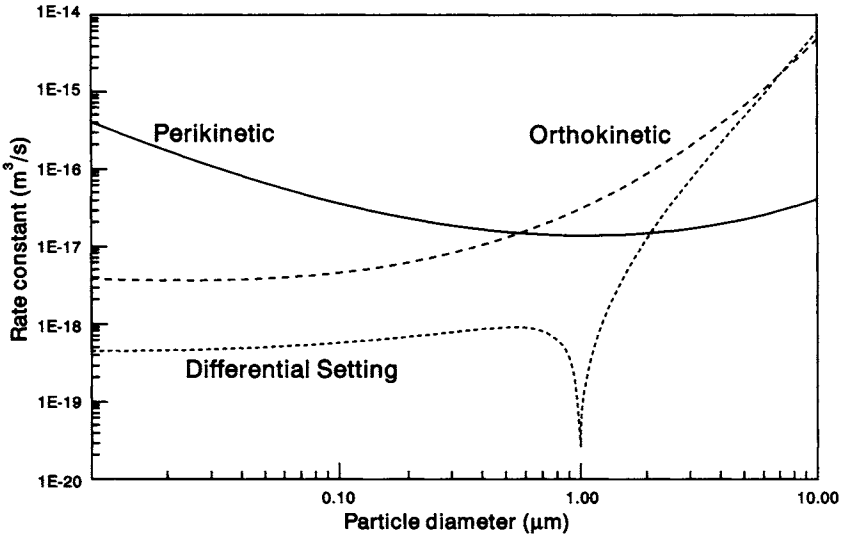

Figure 6.3 *Comparison of collision rate constants for different transport mechanisms (see text)*

The orthokinetic result is for the case of laminar shear, but should also be acceptable for turbulent collisions of particles smaller than the Kolmogoroff microscale. For comparison of these results, it is convenient to take one particle of fixed size and compute the various rate constants as a function of the size of the second particle.

The results of such computations are shown in Figure 6.3, in which one particle is taken to have a diameter of 1 μm and the other diameter varies between 0.01 and 10 μm. The shear rate is assumed to be $50\,s^{-1}$ and the density of the particles $2\,g\,cm^{-3}$. All other values are appropriate for aqueous dispersions at 25°C. It is clear that the perikinetic mechanism gives the highest collision rates for particles less than about 0.6 μm in diameter, but that for larger particles orthokinetic collisions and differential settling become much more important. Note that the perikinetic rate passes through a minimum for equal-size particles, as expected from eqn (6.8). As the size of the second particle becomes greater than a few micrometres, the collision rate due to sedimentation increases sharply and becomes comparable to the shear-induced rate.

Of course, results like those in Figure 6.3 depend greatly on the assumed conditions. Choosing, for instance, a lower density of the particles would give a reduced effect of differential settling. Also, the various collision rate constants are affected in different ways by colloidal and hydrodynamic interactions (see Section 6.3). Nevertheless, the broad conclusions concerning the relative importance of the different mechanisms and the effect of particle size remain essentially correct.

6.3 Collision efficiencies

All of our previous treatment of aggregation rates has been based on the assumption that all particle collisions are successful in producing aggregates. In practice, this is very often not the case and allowance has to be made for the reduced *collision efficiency* (i.e. the fraction of successful collisions). Formally, all that is needed is to incorporate the collision efficiency, α, into the rate expressions discussed earlier. For example, the rate of change of the primary particle concentration, given by eqn (6.10), becomes:

$$\left(\frac{dn_1}{dt}\right)_{t\to 0} = -\alpha k_{11} n_1^2 \tag{6.30}$$

There remains the problem of assigning a value to α and this presents some difficulties. The collision efficiency can be very significantly reduced as a result of repulsive colloidal interactions, such as double layer repulsion or steric interaction (see Chapter 3). Another major effect is due to *hydrodynamic* or *viscous* interaction (Chapter 4), which tends to hinder the approach of colliding particles. Collisions brought about by diffusion or by induced particle motion are affected in different ways by these interactions and a comprehensive treatment is difficult. Initially, we will consider the effect of colloidal interactions on Brownian collisions and then go on to discuss hydrodynamic effects.

6.3.1 Stability ratio – the Fuchs approach

The effect of repulsive colloidal interactions on perikinetic aggregation is to give a reduction in the rate. It is conventional to speak of a *stability ratio*, W, rather than collision efficiency. The stability ratio is simply the ratio of the aggregation rate in the absence of colloidal interactions (i.e. the diffusion-controlled rate) to that found when there is repulsion between particles. It should be clear that W is just the reciprocal of the collision efficiency, i.e. $W = 1/\alpha$.

For cases where only van der Waals attraction and electrical repulsion need to be considered, and there is an energy barrier hindering the close approach of particles (see 3.5.1), the stability ratio can be calculated by treating the problem as one of diffusion in a force field (Fuchs, 1934), in a manner analogous to the treatment of particle deposition by convective diffusion (see 5.5). The result is:

$$W = 2\int_0^\infty \frac{\exp(\phi_T/kT)}{(u+2)^2}\,du \tag{6.31}$$

where ϕ_T is the total interaction at a particle separation distance d, and u is a function of d and particle size. For spherical particles of different radii, a_i and a_j, u is given by:

$$u = \frac{2d}{(a_i + a_j)} \tag{6.32}$$

For equal particles this becomes simply $u = d/a$.

So, to evaluate W, the integral in eqn (6.31) has to be evaluated numerically, using appropriate expressions for the electrical and van der Waals interactions (see Chapter 3). Because of the exponential term, most of the contribution to the integral in eqn (6.31) comes from a region close to the maximum (see Figure 5.7) and a simple approximation due to Reerink and Overbeek (1954) can be used, which for unequal particles becomes:

$$W \approx \frac{1}{\kappa(a_i + a_j)} \exp\left(\frac{\phi_{max}}{kT}\right) \tag{6.33}$$

where κ is the Debye–Hückel parameter and ϕ_{max} is the height of the energy barrier.

Even for quite modest barrier heights, of the order of a few kT units, eqn (6.33) can yield very high stability ratios. Thus, for equal, 1-μm-diameter particles in a 100 mM solution of a 1–1 electrolyte, the term κa is about 500. For a barrier height of $10kT$, the stability ratio would be about 45, and for a $20kT$ barrier W is about 1×10^6 (i.e. only one in every million collisions would occur between particles having sufficient energy to overcome the barrier).

It is not surprising that quite small changes in electrolyte concentration or in surface potential of particles can have dramatic effects on aggregation rates. A quantitative prediction of the effect of (indifferent) salt concentration on stability ratio can be made on the basis of eqn (6.33), assuming simple DLVO-type interaction (Reerink and Overbeek, 1954). It is found that the rate of change of W with salt concentration, when plotted in log–log form, is given by:

$$\frac{d\log W}{d\log c} = -2.06 \times 10^9 \frac{a\gamma^2}{z^2} \tag{6.34}$$

where c is the concentration (mol dm^{-3}) of symmetrical (z–z) electrolyte, a is the particle radius (m) and the numerical constant is appropriate for aqueous dispersions at 25°C. γ is a dimensionless function of the surface potential of the particles, given by:

$$\gamma = \tanh \frac{ze\psi_\delta}{4kT} \tag{6.35}$$

where ψ_δ is the Stern potential and e the electronic charge.

In fact, the stability ratio does not decrease indefinitely as the salt concentration is increased, as implied by eqn (6.34). At a critical concentration, the potential energy barrier just disappears and aggregation should then occur at a transport-limited rate, determined by the collision frequency. At this point, the stability ratio and the collision efficiency should both become unity. This is often called the *critical coagulation concentration* (CCC). The form of the stability ratio versus electrolyte concentration plot is shown in Figure 6.4. Beyond the critical salt concentration there may be significant attraction between the particles, but this is rarely of sufficiently long range to give an appreciable increase in the collision radius of the particles and an enhanced collision frequency.

Experimental values of stability ratio are often found to give an approximately linear decrease with salt concentration on a log–log plot, but the slopes of the

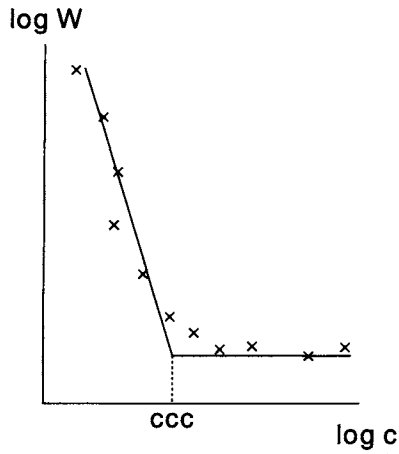

Figure 6.4 *Schematic diagram showing the effect of increasing salt concentration on stability ratio, W. On a log–log plot an approximately linear decrease is found until the critical coagulation concentration is reached, when the stability ratio becomes constant*

lines do not show the dependence on particle size and z predicted by eqn (6.34). Measurement of the aggregation rates of polystyrene latices with different particle sizes showed no systematic dependence on size (Ottewill and Shaw, 1966). Aggregation of negatively-charged silver iodide sols gave slopes which were not very different for La^{3+}, Ba^{2+} and K^+ salts (Frens and Heuts, 1988), despite the predicted dependence on $1/z^2$.

On closer inspection, linear behaviour of $\log W$–$\log c$ plots is difficult to justify on the basis of eqn (6.34), because of the γ^2 term. This means that a linear plot would be expected only if the Stern potential of the particles remained constant over a range of electrolyte concentrations. Judging by the effect of salt concentration on zeta potentials, this is a rather dubious assumption, especially close to the CCC, where there is often a large decrease in zeta potential over quite a small range of salt concentration. Nevertheless, more exact computations of stability ratio, by numerical integration of eqn (6.31) rather than using the approximation in eqn (6.33), give a predicted dependence of stability ratio on salt concentration which is rarely in accord with measured values.

This subject has received a great deal of attention in the colloid literature (Overbeek, 1980) and several suggestions have been made to reconcile measured stability ratios with those predicted on the basis of eqn (6.31). Aggregation in secondary minima, distributions of particle size and surface potential, hydrodynamic effects (see Section 6.3.3) and dynamic effects in double layer interaction (Dukhin and Lyklema, 1990) have all been invoked to account for the discrepancies. Although incorporation of such effects may improve the agreement with measured stability ratios, some uncertainties still remain. The position is rather like the problem of predicting rates of particle deposition in the

presence of a repulsive interaction (see Section 11.1), where measured deposition rates can be very much higher than those computed from convective-diffusion theory.

From a practical standpoint, the lack of quantitative agreement between measured and computed 'slow' aggregation rates may not be of great significance, since the critical salt concentration for rapid (diffusion-limited) aggregation can be fairly well predicted from DLVO theory. Nevertheless, until a satisfactory modelling of 'slow' aggregation has been achieved, our understanding of the phenomena involved will remain incomplete.

6.3.2 Orthokinetic collision efficiencies

For collisions of non-Brownian particles (greater than a few micrometres in size), the Fuchs concept of diffusion in a force field is not appropriate and we have to consider the relative motion of particles induced by fluid shear or by external forces such as gravity. In such cases it may be possible for colliding particles to overcome potential energy barriers as a result of their relative motion. It has been observed that aggregation of otherwise stable colloids can sometimes be achieved by the application of sufficiently high shear. For instance, Zollars and Ali (1986) found that latex particles which were stable against Brownian aggregation for up to 4 years could be coagulated in a few minutes by the shearing at very high rates. The phenomenon of *shear flocculation* (Warren, 1981) is probably an example of such an effect. It should be clear that, for a given suspension, the collision efficiency for Brownian aggregation could be very different from that for orthokinetic collisions. In some cases similar values are found (Swift and Friedlander, 1964), but the agreement is probably fortuitous.

The question of collision efficiency for orthokinetic collisions cannot be adequately discussed without reference to hydrodynamic interaction. This is the subject of the next section.

6.3.3 Hydrodynamic interaction

The Smoluchowski approach to aggregation kinetics takes no account of the effect of the viscosity of the suspending medium on the collision of particles. In fact, *hydrodynamic* or *viscous* effects can have a great effect on aggregation rates. As particles approach very close it becomes increasingly difficult for the liquid between them to drain out of the gap and this tends to slow the aggregation process.

In perikinetic aggregation the effect is manifested as a reduced diffusion coefficient as particles approach close together which can be calculated exactly for the case of equal particles as a function of separation distance (Spielman, 1970). A useful empirical approximation was found by Honig *et al.* (1971):

$$\frac{D(u)}{D(\infty)} \approx \frac{6u^2 + 4u}{6u^2 + 13u + 2} = \frac{1}{\beta(u)} \tag{6.36}$$

where $D(u)$ and $D(\infty)$ are diffusion coefficients for particles separated by a dimensionless distance u $(=d/a)$ and at infinite separation respectively. $\beta(u)$ is

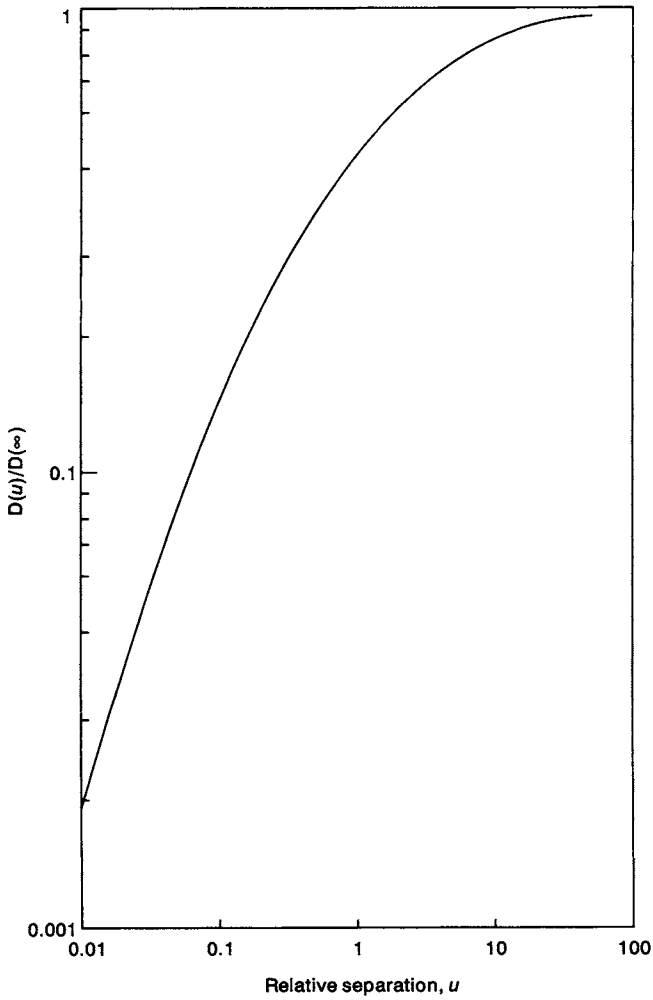

Figure 6.5 *Approximate values of* D(u)/D(∞), *from eqn (6.36), plotted against dimensionless separation distance,* u

the factor by which the diffusion coefficient is reduced at separation u, relative to the value for an isolated particle.

The function $1/\beta(u)$ is plotted against u in Figure 6.5 and it is apparent that the effect is of rather long range, giving an appreciable decrease in diffusion coefficient at separations up to at least 10 times the particle radius. Note also that the diffusion coefficient approaches zero as the particles come into contact, which means that, in the absence of any other interaction, aggregation could not occur. In reality, universal van der Waals attractive forces counteract the

hydrodynamic resistance at close approach and particle contact can be achieved.

The factor $\beta(u)$ can be inserted in the Fuchs expression, eqn (6.31), to give a modified stability ratio. If we assume that the particles are fully destabilized, so that only van der Waals attraction needs to be considered, the following result for the *limiting stability ratio*, W_{lim}, is obtained (Honig *et al.*, 1971):

$$W_{\text{lim}} = 2\int_0^{\infty} \beta(u)\,\frac{\exp(\phi_A/kT)}{(u+2)^2}\,du \tag{6.37}$$

where ϕ_A is the van der Waals interaction energy. Without the exponential term, the integral would diverge, giving an infinite value of the stability ratio.

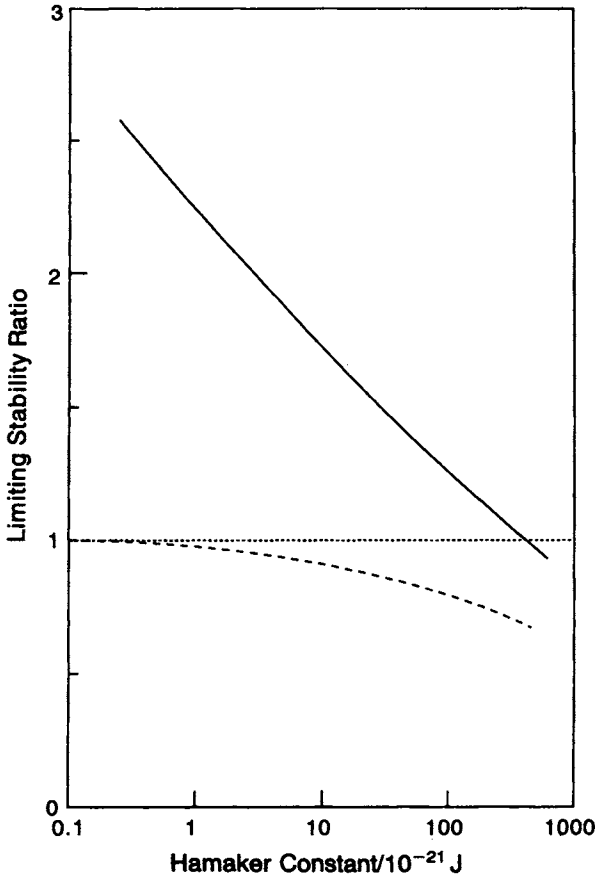

Figure 6.6 *Limiting stability ratio* W_{lim}, *from eqn (6.37), as a function of the Hamaker constant (——). For comparison the result in the absence of hydrodynamic interaction is also shown (---)*

The combined effect of van der Waals and hydrodynamic interactions on the limiting stability ratio of spherical particles in water is shown in Figure 6.6, where W_{lim} is plotted against the effective Hamaker constant. The procedure was to calculate the van der Waals attraction energy, for a given value of Hamaker constant and over a range of particle separations, and to evaluate the integral in eqn (6.37) numerically, using the value of $\beta(u)$ from eqn (6.36). For comparison, the value of W_{lim} in the absence of hydrodynamic interaction (calculated by setting $\beta(u) = 1$) is also plotted in Figure 6.6 (dashed line).

These results show that over the likely range of Hamaker constants ($1–100 \times 10^{-21}$ J), the limiting stability ratio would vary from about 2.3 to 1.2. Only for the improbably high value of $A = 3 \times 10^{-19}$ J would van der Waals attraction entirely cancel out viscous resistance and give $W_{\text{lim}} = 1$. Measurements of perikinetic aggregation rates for latex particles give apparent rate coefficients around half the calculated Smoluchowski value (Lichtenbelt *et al.*, 1974), indicating $W \approx 2$ and a Hamaker constant of about 5×10^{-21} J, in reasonable agreement with accepted values.

In the absence of hydrodynamic interaction, van der Waals attraction has little effect on the stability ratio over the usual range of values. This is because dispersion forces operate over a rather limited range, much less than the particle radius, and so give only a minor increase in the effective collision radius. The larger effect seen in Figure 6.6 when viscous interaction operates arises because van der Waals attraction becomes significant at close approach, where the hydrodynamic effect also becomes very large. The two effects counteract each other to a considerable extent.

Although it needs to be considered, the hydrodynamic effect does not have a dramatic effect on perikinetic aggregation, slowing the rate by a factor of no more than about 2. In the case of *orthokinetic* aggregation, viscous interaction can be much more significant.

The Smoluchowski treatment of orthokinetic collision rate assumes that particles in a uniform shear field move along straight streamlines until they collide with another particle (see Figure 6.2). In reality, streamlines curve around obstacles such as other particles, which makes collision less likely. The conventional 'no slip' assumption implies that, in the absence of any other effect, particles could not come into contact as a result of fluid motion, because the last layer of liquid between them could not be removed by viscous flow. Brownian motion and the presence of attractive interparticle forces allow aggregation to occur.

A full treatment of this problem involves computing trajectories of particles, incorporating hydrodynamic and colloidal interactions. It is convenient to consider a reference sphere at the centre of the coordinate system and compute the number of other particles colliding with this in unit time. By finding the 'limiting trajectory', which just brings a particle into contact with the reference particle, and tracing this trajectory back to a point far upstream, an orthokinetic collision efficiency can be calculated. This is the fraction of particles approaching within a cylinder defined by the collision radius (Figure 6.2) which collide with the reference particle. The method is similar to the trajectory analysis discussed in Section 5.6 for particle deposition on collectors.

Van de Ven and Mason (1977) used such an approach, incorporating van der Waals attraction and double layer repulsion. In the absence of repulsion, a *limiting collision efficiency*, α_0, was derived. This is defined in such a way that the collision frequency can be obtained simply by multiplying the appropriate Smoluchowski result by α_0. Thus, for equal particles of radius a and concentration n, the collision frequency, J, is:

$$J = \frac{32}{3} \alpha_0 n^2 G a^3 \tag{6.38}$$

This is obtained directly from eqn (6.19), by setting n_i and n_j equal to n, and a_i and a_j to a.

The computed results of van de Ven and Mason are well represented by a simple empirical expression:

$$\alpha_0 = f(\lambda/a) C_A^{0.18} \tag{6.39}$$

where $f(\lambda/a)$ is a function of the dispersion wavelength (since retardation effects were included) and the particle size, for which some values were given, and C_A is given by:

$$C_A = \frac{A}{36\pi\mu G a^3} \tag{6.40}$$

This expression shows that the collision efficiency decreases as the particle size and the shear rate increase. The dependence on shear rate means that the collision frequency varies as $G^{0.82}$, rather than being linearly dependent on shear rate, as in the Smoluchowski result.

Taking $A = 10^{-20}$ J, $\lambda = 100$ nm and $\mu = 10^{-3}$ Pa s as reasonable values for aqueous suspensions, values of α_0 can be calculated for different particle sizes and for different shear rates. In Figure 6.7 the limiting collision efficiency is plotted as a function of shear rate for three different particle sizes (1 μm, 2 μm and 4 μm diameter). The implication of these results is that, as aggregates grow, especially at high shear rate, there will be a corresponding decrease in α_0, which will tend to restrict further aggregation. However, the collision rate increases for larger particles, eqn (6.19), so that the aggregation rate may not be greatly affected.

The results just discussed are for colliding particles of equal size. For *unequal* particles, collision efficiencies can become very low (Adler, 1981). It is found that in some cases the trajectory of a smaller particle around a larger one is such that a large separation between the particles is maintained, with virtually no chance of capture. For instance, for particles with radii of 10 μm and 1 μm, the distance of closest approach has been calculated to be about 1.4 μm (van de Ven and Mason, 1981). This is far greater than the range of van der Waals attraction and it is difficult to see how any aggregation could occur in such cases. Brownian motion and the porous nature of aggregates may modify this conclusion. All real aggregates have a rather open structure and it is very likely that hydrodynamic resistance is greatly reduced when the approaching surfaces are permeable to the liquid.

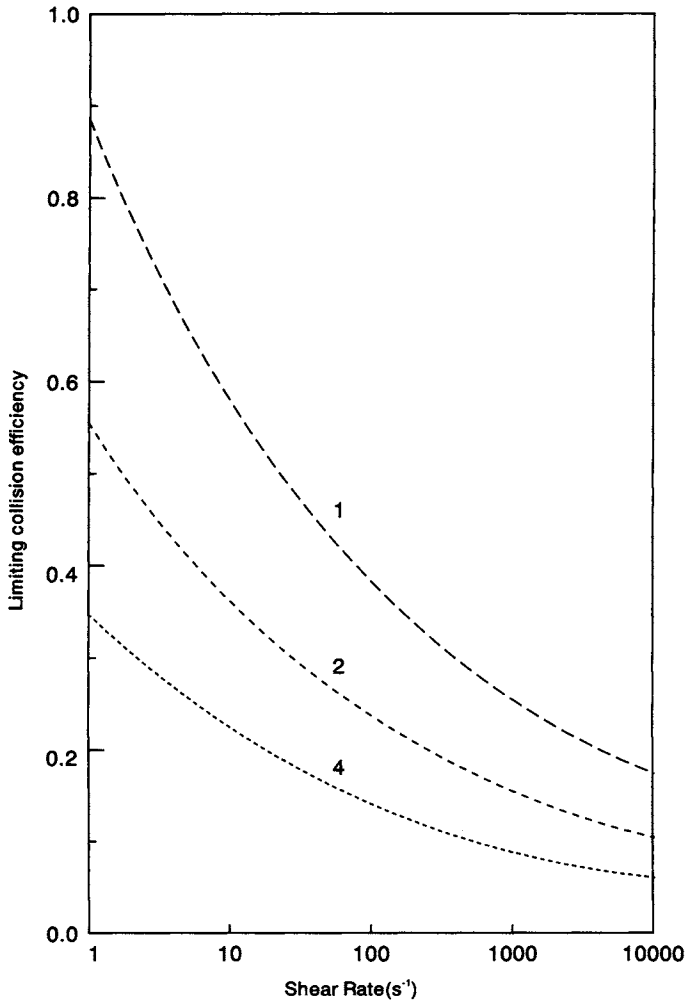

Figure 6.7 *Limiting collision efficiencies, for orthokinetic aggregation of fully destabilized particles, as a function of the applied shear rate. The colliding particles are assumed to be equal spheres with diameters (μm) shown on the curves*

In the presence of double layer repulsion the computations of van de Ven and Mason (1977), for equal spheres, show rather complex behaviour. Depending on conditions, particles may be stable or may aggregate into primary or secondary minima. It is possible that a suspension may be stable over a certain range of shear rates, but aggregate at higher and lower values. For aggregation into a secondary minimum, high shear rates would tend to pull aggregated particles apart. However, high shear rates can increase the chance of colliding particles

overcoming a potential energy barrier and being captured in a primary minimum. Predictions of such behaviour in real systems are severely limited by the lack of detailed information on the relevant colloidal interactions and the appropriate parameters (zeta potentials, Hamaker constants, adsorbed species, etc.). Quite small changes in the assumed parameters can have very large effects on the computed results.

In the case of differential sedimentation, the effect of hydrodynamic interaction on aggregation rate has been analysed by Melik and Fogler (1984).

Hydrodynamic interaction affects the different aggregation mechanisms to different extents and will modify the previous discussion based on Figure 6.3, especially for particles larger than about 2 μm. Nevertheless, the qualitative conclusions concerning the relative importance of the different types of collision process remain broadly correct.

6.4 Form of aggregates

When solid particles aggregate, no coalescence can occur and the resulting clusters may adopt many different forms. In the simplest case of equal spheres, there is no doubt about the shape of a doublet, which must be in the form of a dumbbell. However, a third particle can attach in several different ways and with higher aggregates the number of possible structures rapidly increases, as indicated in Figure 6.8. In real aggregation processes, aggregates containing hundreds or thousands of primary particles can arise and it will never be possible

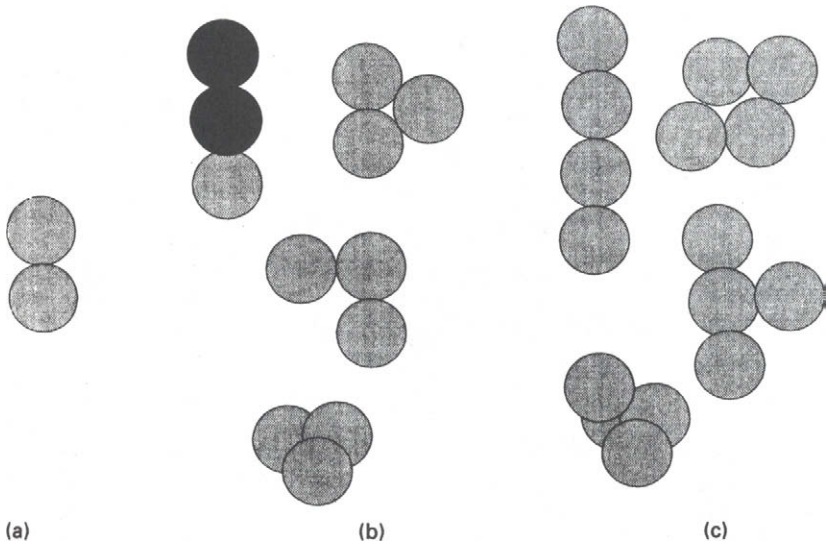

Figure 6.8 *Showing possible forms of aggregates of equal spheres:* (a) *doublets,* (b) *triplets, and* (c) *quadruplets*

to provide a detailed description of their structure. Some convenient method is needed which enables aggregate structure to be characterized in general terms, but still conveys useful information. A great deal of progress was made in this area during the 1980s, largely as a result of computer simulation of aggregate formation and the study of model aggregates.

6.4.1 Model studies: fractal clusters

Aggregates are now recognized as *fractal objects* (Meakin, 1988). If, for a large number of aggregates, the mass is plotted against aggregate size (diameter, for example), the plot may be linear, but with a non-integer slope. (For regular, three-dimensional objects the slope of such plots is 3.) For aggregates, the slope of the line, d_F, is called the *fractal dimension*, and can be considerably less than 3. There are several other ways of defining fractal dimension. Strictly, d_F should be called a *mass fractal dimension*, but the general term will be used here. The lower the fractal dimension, the more open (or 'stringy') is the aggregate structure. The relationship between aggregate mass, M, and size, L, is just:

$$M \propto L^{d_F} \tag{6.41}$$

The 'size' L can be defined in various ways and in fundamental studies it is often taken as the radius of gyration of the aggregate. However, the precise definition of L does not affect the form of eqn (6.41) and it may be convenient to use the largest diameter of an irregular aggregate as the measure of its size. If the relationship in eqn (6.41) applies over a wide range of aggregate sizes, then it implies that the aggregates have a *self-similar* structure, which is independent of the scale of observation (or the degree of magnification). This concept is illustrated schematically in Figure 6.9, where the fundamental unit is assumed to be a triplet of equal spheres. This simple two-dimensional illustration is not intended to represent real aggregates, but only to convey the idea of self-similarity. It is reminiscent of earlier ideas (e.g. Michaels and Bolger, 1962) on the 'hierarchical' nature of aggregation, in which small aggregates combine to form larger 'flocs'. Such models were normally restricted to just a few discrete levels of aggregation, rather like the simple picture in Figure 6.9. The essence of self-similar aggregates is that there is a continuum of 'levels' from large-scale structures down to individual primary particles.

Computer modelling of aggregation has given very useful insights into the process. Early studies were based only on the random addition of single particles to growing clusters (Vold, 1963). Later simulations (Meakin, 1988) of diffusion-controlled (i.e. 'rapid' perikinetic) aggregation, with single-particle addition (diffusion-limited aggregation), gave fairly dense structures, with d_F about 2.5. In many cases, single-particle addition is not a realistic model, since, throughout most of an aggregation process, growth occurs as a result of cluster–cluster encounters. In this case, computer simulations and experimental studies on a range of model colloids (Lin *et al.*, 1989) show much more open structures with a fractal dimension of around 1.8. It is important to realize that these simulations are based on the assumption that particles attach permanently to other particles

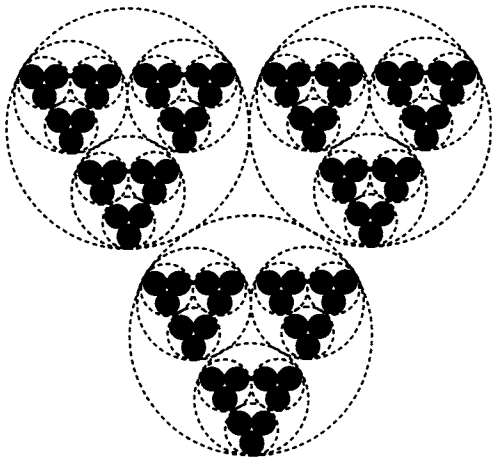

Figure 6.9 *Schematic illustration of self-similar aggregate structure*

at the first contact; the process is controlled entirely by diffusion – hence 'diffusion-limited aggregation' (DLA).

Intuitively, there is a simple reason for the difference in structure of aggregates produced by particle–cluster and cluster–cluster aggregation, illustrated in Figure 6.10. In the former case, a particle is able to penetrate some way into a cluster before encountering another particle and sticking. In an encounter of two clusters the first contact is likely to occur before the clusters have interpenetrated to a significant extent, which leads to a much more open structure.

When there is interparticle repulsion, so that the collision efficiency is reduced, aggregation is then said to be 'reaction-limited' and very different aggregate structures can be obtained under these conditions. It is found (Lin *et al.*, 1989) that reaction-limited aggregates are more compact than those produced by DLA, with a fractal dimension $d_F \approx 2.1$, for the cluster–cluster case. Again, it is not difficult to find an explanation for this effect. When the collision efficiency is low, particles (or clusters) need to collide many times before sticking occurs. This gives more opportunity to explore other configurations and to achieve some degree of interpenetration.

Less attention has been paid to aggregates produced by mechanisms other than diffusion. There is evidence that 'ballistic' aggregation (where encounters occur as a result of linear trajectories) gives rather more compact structures, especially in the particle–cluster case, where d_F can approach a value of 3. In the cluster–cluster case simulations of ballistic aggregation give $d_F \approx 1.9$ (Tence *et al.*, 1986). It is not clear how ballistic aggregation relates to shear-induced collisions and orthokinetic aggregation. Torres *et al.* (1991b) have simulated aggregation in viscous flows and found that aggregates produced by cluster–cluster encounters in shear and extensional flow are very like those formed by DLA, with $d_F \approx 1.8$. For particle–cluster aggregation, much more compact structures result with d_F

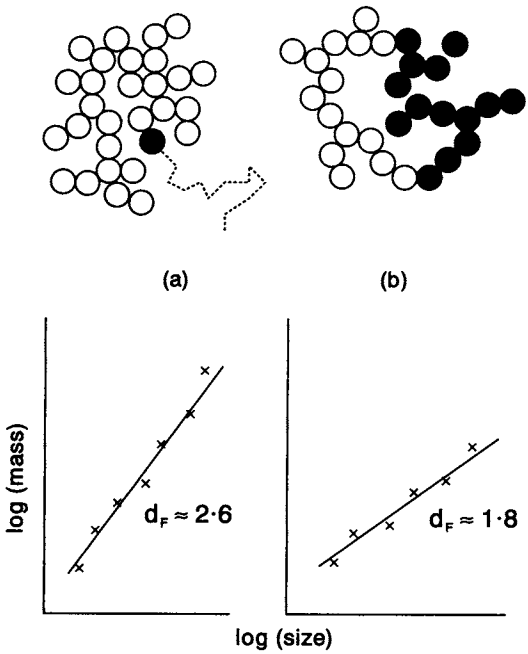

Figure 6.10 *Fractal aggregates produced by* (a) *single-particle addition to an aggregate and* (b) *cluster–cluster aggregation. In the latter case, aggregates are more open in structure and have a lower fractal dimension,* d_F

values up to about 2.9, although there is some dependence on the nature of the flow.

Measurements of fractal dimensions of aggregates formed from colloidal nickel hydroxycarbonate have been reported by Hoekstra *et al.* (1992), for both perikinetic and orthokinetic aggregation and for high and low colloid stability. Although their systems were far from 'ideal', the results were broadly in line with previous model studies and simulations. For rapid, diffusion-controlled aggregation, a fractal dimension of 1.7–1.8 was found. At low salt concentration, where aggregation was reaction limited, d_F was in the region of 2.0–2.1. For orthokinetic aggregation (in Couette flow) at high salt concentration, d_F was found to be shear-dependent, increasing from 1.7 at zero shear to about 2.2 at a shear rate of 200 s^{-1}. For orthokinetic collisions under reaction-limited (low-salt) conditions, fractal dimensions up to 2.7 at 200 s^{-1} were found.

The assumption so far that contacts between particles, once formed, are permanent, means that aggregates cannot undergo any subsequent restructuring. In fact, changes in aggregate structure have often been observed, always giving more compact forms (higher d_F). For example, Aubert and Cannell (1986) found that coagulation of silica particles under diffusion control initially gave

aggregates with $d_F \approx 1.75$, but, after a few hours, these became more compact, with $d_F \approx 2.1$, which is the value achieved by reaction-limited aggregation.

It is very likely that agitation, as in stirred vessels, is effective in giving some compaction of flocs (higher d_F), probably by causing some deformation and rearrangement. This is a subject of great practical interest, but it has not received much fundamental attention.

6.4.2 Aggregate density

A very important consequence of the fractal, self-similar nature of aggregates is that their density decreases appreciably as the size increases. Actually, such behaviour had been empirically observed well before the concept of fractal aggregates was introduced. Lagvankar and Gemmell (1968) found that flocs produced under water treatment conditions had effective densities that decreased markedly with increasing size. Similar observations had been made in Japan from the 1960s by Tambo and coworkers (Tambo and Watanabe, 1979).

The effective, buoyant density of an aggregate in a liquid, ρ_E, is simply:

$$\rho_E = \rho_F - \rho_L = \phi_S(\rho_S - \rho_L) \tag{6.42}$$

where ρ_S, ρ_L and ρ_F are the densities of the solid particles, the liquid and the aggregate (floc), respectively, and ϕ_S is the volume fraction of solid in the floc.

Since most measurements of floc density involve some form of sedimentation procedure, the buoyant density, ρ_E is the relevant property. When ρ_E is plotted against the floc diameter, in log–log form, a linear decrease is often found, implying a relationship of the form:

$$\rho_E = Ba^{-y} \tag{6.43}$$

where B and y are constants.

Because of the proportionality between ρ_E and ϕ_s, it follows that the exponent y is related to the fractal dimension:

$$d_F = 3 - y \tag{6.44}$$

Measurements of aggregate densities for many suspensions of practical interest, including mineral particles, sewage sludges and aluminium hydroxide flocs, give y values in the range 1–1.4, corresponding to fractal dimensions of 2–1.6, which are in line with those obtained by simulation and in model systems. This lends considerable support to the idea of 'universality' in particle aggregation (Lin *et al.*, 1989).

The values of y quoted above imply a very substantial decrease in density with increasing floc size. With $y = 1.2$ ($d_F = 1.8$), a 10-fold increase in size gives a 16-fold reduction in the effective floc density. Assuming that Stokes' law holds, the corresponding increase in sedimentation rate would be by a factor of less than 6, rather than the 100-fold increase that would be expected on the basis of constant floc density. So, the fractal nature of flocs has very important implications for gravitational or centrifugal separation processes.

Other solid–liquid separation processes are also affected by the density of flocs. Dewatering operations proceed more rapidly when flocs are more compact since, effectively, there is less solid surface in contact with water and hence less drag. Also, more open, low-density flocs are more likely to be compressed during cake filtration and this can lead to blocking of pores and a reduced filtration rate. It is very significant that substantial improvements in filterability of flocs can be achieved by recirculation of flocculated solids (Knocke and Kelley, 1987). In this way newly-introduced, unflocculated particles are brought into contact with preformed flocs and aggregation of the particle–cluster type would be expected. From simulation studies, this is known to produce more compact aggregates than cluster–cluster processes. The higher density of flocs formed in upflow clarifiers, where incoming particles flow through a layer of preformed floc, can probably be explained by essentially the same reasoning.

In some cases, lower density flocs might be preferred. For instance, the capture of particles in granular filters and in orthokinetic flocculation is greatly dependent on the effective collision radius, which, for a given degree of aggregation, will become greater as the floc density decreases. The effect of the fractal nature of aggregates on aggregation kinetics will be briefly discussed in the next section.

6.4.3 Collision rates of fractal aggregates

The Smoluchowski treatment of aggregation kinetics is based on the assumption that the colliding particles are spheres. Even for spherical primary particles, aggregation quickly leads to shapes like those in Figure 6.8, and their collision rates cannot be calculated exactly. Only in the case of coalescing liquid droplets could the assumption of spherical particles be justified.

For perikinetic aggregation, the growth of aggregates gives an increasing collision radius and a reduced diffusion coefficient and these effects tend to cancel out, giving a collision rate constant which is not greatly dependent on aggregate size. For fractal aggregates, the hydrodynamic radius (which determines the drag and hence the diffusion coefficient) is likely to be somewhat less than the outer 'capture radius', corresponding to the physical extent of the aggregate. For high degrees of aggregation, the ratio of these two radii has been calculated to be about 0.6 (Torres *et al.*, 1991a). This means that Brownian collisions will occur rather more rapidly than predicted from the rate constant in eqn (6.9). However, for aggregates greater than a few micometres in size, perikinetic aggregation is negligible and collisions induced by shear become far more important.

In the orthokinetic case, it is the effective capture radius of a fractal aggregate that is of paramount importance and this is greatly dependent on the fractal dimension (e.g. Wiesner, 1992). Instead of eqn (6.20), the collision rate constant for orthokinetic collisions between i and j particles can be written:

$$k_{ij} = \frac{4Ga_0^3}{3}(i^{1/d_F} + j^{1/d_F})^3 \tag{6.45}$$

where a_0 is the radius of the primary particles and it has been assumed that the radius of an i-fold aggregate is given by:

$$a_i = a_0 i^{1/d_F} \tag{6.46}$$

by analogy with the definition of fractal dimension in eqn (6.41).

For the 'coalesced sphere' assumption, $d_F = 3$, and the increase in aggregate size is relatively slow (a 10-fold increase in capture radius for 1000-fold aggregates). For lower values of d_F, the aggregate size increases more rapidly, which can give a dramatic increase in aggregation rate (Jiang and Logan, 1991). The implications for the evolution of aggregate size distribution have been discussed by Wiesner (1992). An obvious consequence of the fractal nature of aggregates is that the effective floc volume will not be conserved, as assumed in the derivation of eqn (6.23). There will be a substantial increase in floc volume for typical values of d_F and this is the reason for the increased collision frequency.

Another very important outcome of the fractal nature of aggregates is that hydrodynamic interaction is much less significant than for solid particles and the very large effects expected for unequal-size particles (Section 6.3.3) are not found for aggregates. Torres *et al.* (1991a) calculated stability ratios for aggregates in shear flow and found values only slightly in excess of 1. It should be clear from the simple pictures in Figure 6.10 that particle–cluster and cluster–cluster collisions will be hindered much less by hydrodynamic effects than would similar encounters involving solid particles equivalent in size to the clusters.

6.5 Aggregate strength and break-up

It was stated at the beginning of our discussion of aggregation kinetics that aggregation would be regarded as irreversible, and this assumption is implicit in expressions such as eqn (6.2). This is a convenient assumption, since the break-up of aggregates is very difficult to model. However, since nearly all aggregation processes are carried out with some form of agitation, the break-up process cannot be ignored. In practice, it is often found that aggregates (flocs) reach a certain, limiting size, which depends on the applied shear or energy dissipation and on the *floc strength*. Empirically, the size may depend on the energy dissipation according to (e.g. Mühle and Domasch, 1991):

$$d_{max} = C\epsilon^{-n} \tag{6.47}$$

where C and n are constants.

There are several theoretical approaches for floc break-up in turbulent flow which lead to expressions of the form of eqn (6.47) (Tambo and François, 1991; Mühle, 1993). The exponent depends on the size of the floc relative to the turbulence microscale; for instance, for flocs large compared to the microscale an exponent of around -0.4 may be found, whereas for much smaller flocs the dependence on energy input is not so great and $n \approx 0.3$. However, these values are difficult to check experimentally and may be highly system-specific. As a convenient rule of thumb, it is sometimes assumed that the limiting floc size in a turbulent flow field is of the same order as the Kolmogoroff microscale, given by eqn (6.27).

Even in laminar shear, it is not easy to predict maximum aggregate size. Torres *et al.* (1991a) used the following expression to model break-up of large flocs in simple shear, derived by balancing the van der Waals force between two particles with the hydrodynamic force acting to separate two aggregates:

$$(R_{Hi} + R_{Hj}) = \left(\frac{A}{18\pi\mu G a \delta^2}\right)^{1/2} \tag{6.48}$$

where R_{Hi} and R_{Hj} are the dimensionless hydrodynamic radii of two colliding aggregates (scaled by the primary particle radius, a), A is the Hamaker constant and δ is the separation of particles in the primary minimum.

The parameter δ is subject to considerable uncertainty and is often treated as a fitting parameter, with a value of the order of 1 nm or less. Although eqn (6.48) applies to simple shear and is based on simplifying assumptions, it does highlight some important factors governing aggregate strength. For instance, the maximum floc size is predicted to vary as $G^{-0.5}$, which is equivalent to a dependence on $\epsilon^{-0.25}$, and this exponent is of the same order as those found experimentally in some cases (Tambo and François, 1991).

The criterion for limiting floc size in eqn (6.48) is based on the assumption that a collision between two aggregates can only lead to attachment if the sum of their hydrodynamic radii does not exceed a certain critical value. For larger aggregates, the shear force tending to separate them is greater than the binding force. This is equivalent to finding the size of colliding aggregates, under given shear conditions, for which the collision efficiency becomes zero. Such an approach was adopted by Brakalov (1987) for turbulent conditions and the predictions of his model agree quite well with measurements on aggregates of metal hydroxides.

However, there are many cases where the concept of a limiting size based on a vanishing collision efficiency is not appropriate. For instance, aggregates formed under low-shear conditions may break when subjected to higher shear. In that case, floc breakage may occur in several ways, not necessarily into the aggregates from which the floc was formed at the last collision. Experimental observations (e.g. Glasgow and Liu, 1991) indicate that floc breakage is a complex phenomenon, with large-scale fragmentation as well as surface erosion of small components occurring simultaneously. At present, there is no satisfactory model to account for the observed effects, and progress is hampered by the lack of an accepted experimental method for studying floc breakage. Also there is no widely accepted definition of common terms such as 'floc strength'.

Intuitively, the strength of an aggregate must depend on the attractive forces between component particles and the number of particle–particle contacts. The latter must depend on the density of the aggregate, which determines the effective 'coordination number' of the component particles. Because of the fractal nature of aggregates, an increase in size means a decrease in density and a reduced number of particle–particle contacts per unit volume of aggregate. Since the disruptive force increases with size, the limiting size may be reached when the aggregation *number* is still quite small. The same number of primary particles in a smaller, more compact aggregate could be said to be 'stronger' in that it resists a shearing force which would disrupt the larger, lower density aggregate. For this

reason, assessment of 'floc strength' on the basis of the limiting hydrodynamic size achieved under given shear conditions may be misleading. Information on the *mass* of the aggregate would also be relevant.

Inclusion of floc break-up in modelling of aggregation processes usually involves an assumption of the limiting aggregate size under given conditions. Aggregates exceeding this size are assumed to break into two or more 'daughter' aggregates and the precise form of breakage assumed can greatly influence the computed aggregate size distribution.

6.6 Aggregate size distributions

6.6.1 Analytical approaches

There has been a great deal of fundamental interest in solving the Smoluchowski equation, eqn (6.2), to obtain an aggregate size distribution as a function of time. The form of the expression in eqn (6.2) is for *discrete* particle sizes, but an equivalent form can be written for *continuous* particle size distributions (e.g. Rosen, 1984):

$$\frac{\partial n(i,t)}{\partial t} = \frac{1}{2}\int_0^i k(i-j,j)n(j,t)n(i-j,t)\mathrm{d}j - n(i,t)\int_0^\infty k(i,j)n(j,t)\ \mathrm{d}j \qquad (6.49)$$

where the left-hand side represents the rate of change of concentration of particles of size (volume) i and the coefficients $k(j,i-j)$ are equivalent to the collision rate constants k_{ij} etc. in eqn (6.2). In integral expressions these are known as collision *kernels*.

Solution of these expressions is made very difficult by the fact that the collision kernels depend on the size of the colliding aggregates, and the dependence on size is not generally known, except in very simple cases.

The simplest possible assumption is that the collision kernels are constant, independent of size, and in this case eqn (6.49) leads to a very simple form of aggregate size distribution (Meesters and Ernst, 1987). This is most conveniently expressed in terms of a dimensionless aggregate size, x, normalized by the average size, such that, for an aggregate of volume v, the dimensionless size is given by:

$$x = \frac{v}{\bar{v}} = \frac{k}{\bar{k}} \qquad (6.50)$$

where $\bar{v}$ is the average aggregate volume and $\bar{k}$ is the number of primary particles in an aggregate of average volume. As before, the volume of an aggregate is determined by the number of primary particles it contains, so that the average, $\bar{k}$, is given by:

$$\bar{k} = \frac{n_0}{n_T} \qquad (6.51)$$

where, as before, n_0 and n_T are the concentrations of primary particles and *total* particles, respectively.

With this definition, and appropriate initial conditions, the solution of eqn (6.49) turns out to have a simple exponential form. In terms of dimensionless size, x, the size distribution for the constant-kernel case can be written (Meesters and Ernst, 1987):

$$f(x) = \exp(-x) \tag{6.52}$$

where $f(x)$ is the frequency function, such that the fraction of aggregates with (reduced) sizes in the range x to $x + dx$ is $f(x)\,dx$.

The assumption of constant collision kernel is essentially that made by Smoluchowski in deriving the aggregate size distribution in eqn (6.17) for the discrete, perikinetic case. In fact, for long times ($t \gg \tau$), the Smoluchowski result, expressed in dimensionless form, approaches the exponential distribution given by eqn (6.52), as shown in Figure 6.11. In this figure, the points represent aggregate size distributions derived from eqn (6.17), for different reduced times (t/τ) and expressed in terms of the average aggregate size given by eqn (6.51). (For reduced times of 1, 5 and 10, values of $\bar{k}$ are 2, 6 and 11, respectively.) For reduced times greater than 5 and for aggregates larger than the average size ($x > 1$), the points lie close to the exponential result.

Of course, in many practical cases, especially for orthokinetic aggregation, the collision kernels depend greatly on aggregate size and cannot be treated as constant. In order to solve eqn (6.49) for non-constant kernels, it is convenient to

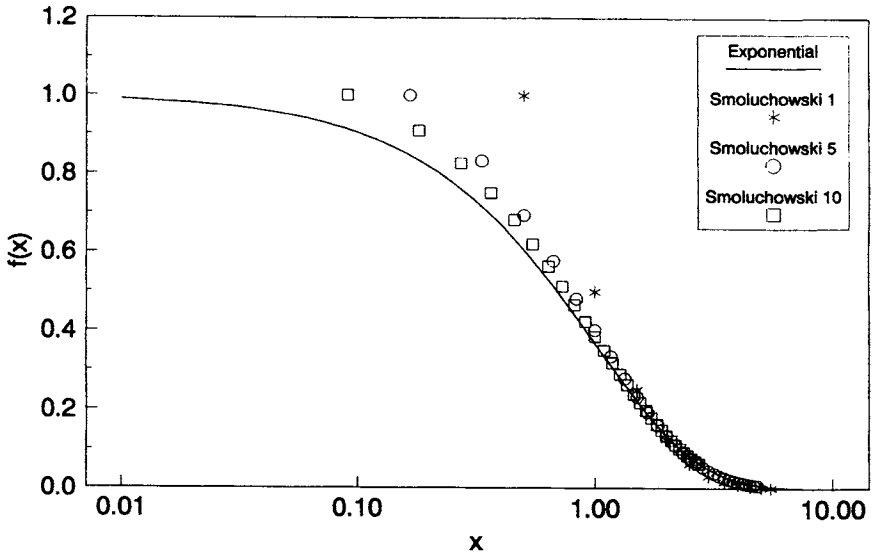

Figure 6.11 *The aggregate size distribution,* f(x), *in terms of the reduced size,* x. *The points are derived from the Smoluchowski expression, eqn (6.17), at different values of the reduced time* (t/τ): *1, 5 and 10. The drawn line is the exponential distribution, eqn (6.52)*

assume that the kernels are homogeneous functions of aggregate size, so that, if the aggregates are increased in size by a certain factor, m, then the kernel increases by a factor m^w, where w is the *degree of homogeneity*:

$$k(mi,mj) = m^w k(i,j) \tag{6.53}$$

When $w=0$ (the constant-kernel case), the exponential form, eqn (6.52), is recovered. For $w>0$, different forms are obtained, typically bell-shaped curves as shown by numerical computations of Meesters and Ernst (1987). The reason is that, for $w>0$, collisions between large and small aggregates (or primary particles) occur more rapidly than in the constant-kernel case, so that small aggregates are less likely to remain. This extra depletion of the smaller aggregates gives bell-shaped, rather than exponential, distributions.

6.6.2 'Self-preserving' distributions

Solution of eqn (6.49) is made much easier if some 'universal' or 'scaling' form is assumed. The first example of such an approach was the 'self-preserving' distribution of Swift and Friedlander (1964), discussed further by Friedlander (1977). This is based on the assumption that the fraction of aggregates in a size range dv is a function only of the dimensionless size, x, defined in eqn (6.50). Thus:

$$\frac{n\,\mathrm{d}v}{n_\mathrm{T}} = f\left(\frac{v}{\bar{v}}\right)\mathrm{d}\left(\frac{v}{\bar{v}}\right) = f(x)\,\mathrm{d}x \tag{6.54}$$

This can be rearranged, using the fact that the average aggregate volume, $\bar{v}$, is simply given by $\bar{v}=v_\mathrm{T}/n_\mathrm{T}$, to give:

$$n(v,t) = \frac{n_\mathrm{T}^2}{v_\mathrm{T}} f(x) \tag{6.55}$$

There are also the integral relations which give the total number of particles, n_T and the total volume of particles, v_T, per unit volume:

$$n_\mathrm{T} = \int_0^\infty n\,\mathrm{d}v \tag{6.56}$$

and:

$$v_\mathrm{T} = \int_0^\infty nv\,\mathrm{d}v \tag{6.57}$$

For a closed system, v_T remains constant and n_T decreases with time.

The implication of these expressions is that, if a form of the aggregate size distribution is known for particular values of n_T and v_T, then the distribution for another value of n_T (i.e. at another time) can be determined from eqn (6.54). When plotted in suitable form, the shapes of the distributions at different times are similar and hence the distribution is said to be 'self-preserving'.

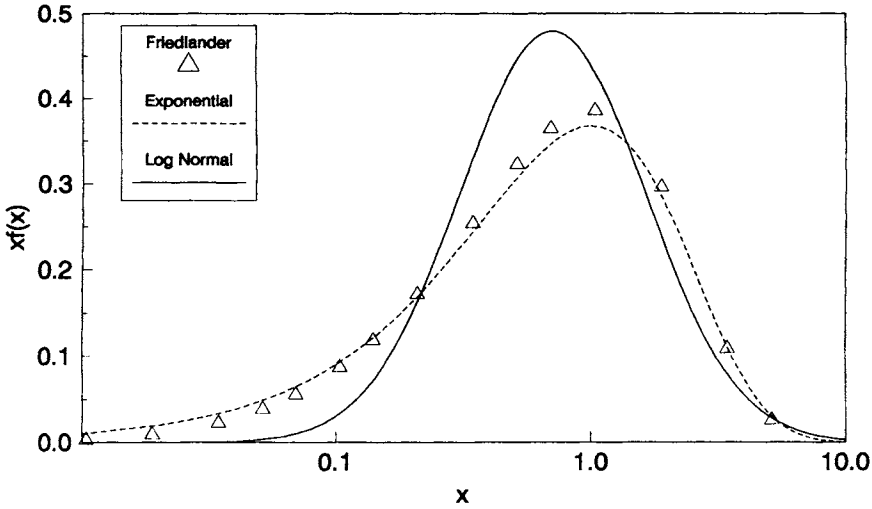

Figure 6.12 *Comparison of 'self-preserving' distributions, in terms of the reduced aggregate size,* x, *as* x f(x) *versus* x. *The results are from the computations of Friedlander and Wang (1966), the exponential form and the log-normal distribution of Lee (1985), eqn (6.59)*

Friedlander and Wang (1966) showed how the integral form of the Smoluchowski expression, eqn (6.49), together with the scaling relation eqn (6.55) and the integral relations above, could be used to derive a numerical solution for Brownian aggregation. The kernels used were from eqn (6.8), so that the dependence on aggregate size is included. The self-preserving distribution obtained in this way is plotted in Figure 6.12, as $x f(x)$ versus x, and appears to be approximately exponential in form.

An alternative approach to Brownian aggregation proposed by Lee (1983, 1985) is to *assume* a log-normal form for the aggregate size distribution and to compute the parameters of the distribution using kernels of the form given by eqn (6.8). Lee showed that the distribution of aggregate sizes tended to a universal form at long times, depending on the breadth of the initial distribution but typically of the order of 10–200 τ (the characteristic aggregation time defined in eqn (6.15)).

The log-normal distribution, expressed in terms of aggregate volume, is written by Lee as:

$$\frac{n(v,t)}{n_T} = \frac{1}{3\sqrt{2\pi}\, v \ln \sigma} \exp\left[\frac{-\ln^2 (v/v_g)}{18 \ln^2 \sigma}\right] \tag{6.58}$$

where $v_g(t)$ is the number median particle volume and $\sigma(t)$ is the geometrical standard deviation based on the aggregate *radius*. This is the reason for the

presence of the factors 3 and 18 on the right-hand side of eqn (6.58), instead of the more familiar values 1 and 2, which appear when the entire distribution is given in terms of particle radius. Note that there is an implicit assumption that $d_F = 3$ and so the aggregates do not have fractal character.

Lee (1985) showed that the value of σ approached a limiting value of 1.32 after long times and that the volume distribution in reduced form could be written:

$$x f(x) = \frac{1}{\sqrt{2\pi \ln 2}} \exp\left[\frac{-(\ln \sqrt{2}\, x)^2}{\ln 4}\right] \tag{6.59}$$

This result is also plotted in Figure 6.12, for ease of comparison with the Friedlander 'self-preserving' distribution. The two curves are seen to be broadly similar, but with peaks at rather different sizes. There is no *a priori* reason to suppose that the distribution will follow the log-normal form and Lee's result has less fundamental justification than that of Friedlander. Nevertheless, log-normal distributions are widely employed and have convenient mathematical properties, so that eqn (6.59) has some attraction.

An interesting consequence of the log-normal result is that the total particle concentration can be shown to vary with time as:

$$\frac{n_T}{n_0} = \frac{1}{1 + 1.04 k_a n_0 t} \tag{6.60}$$

where $k_a = 4kT/3\mu$ (see eqn (6.13)). This differs very little from the Smoluchowski result, eqn (6.14).

Our discussion of limiting or 'self-preserving' distributions has only been concerned with closed systems, where the total number of primary particles remains constant. Steady-state size distributions of environmental particles (e.g. in lakes) are affected by input of particles and loss by sedimentation (e.g. Jiang and Logan, 1991). This aspect will not be considered here.

6.6.3 The 'maximum entropy' approach

Another way of looking at aggregate size distributions is to consider the *most probable* way in which primary particles are distributed among aggregates of different size. For a fixed number of primary particles, n_0, (i.e. for a closed system) and a *total* number of particles n_T in unit volume of suspension, the average aggregate size is n_0/n_T, as in eqn (6.51), and the reduced aggregate size, x, is given by eqn (6.50). If we consider the number of ways in which n_0 primary particles can be distributed among n_T objects, it is possible to find the distribution which represents the maximum number of possible arrangements of particles among aggregates. This is essentially a statistical-mechanical approach and is equivalent to finding the *maximum entropy* of the distribution

(Rosen, 1984). The entropy (or uncertainty), S, of the distribution $f(x)$ is given by:

$$S = \int_0^\infty f(x) \ln f(x) \, dx \tag{6.61}$$

When this function is maximized, using the constraints in eqns (6.56) and (6.57), it turns out that the most probable distribution is given simply by (Rosen, 1984):

$$f(x) = \exp(-x) \tag{6.62}$$

which is just the same as the expression derived analytically for the constant-kernel case, as discussed in Section (6.6.1). For comparison with the Friedlander and log-normal 'self-preserving' distributions, the exponential distribution is also plotted in Figure 6.12 as $x f(x)$ versus x.

It is worth remembering that no assumption about the collision process is made in deriving eqn (6.62) and yet a distribution very like the Smoluchowski result emerges.

Another approach to the most probable distribution (Botet and Jullien, 1984) uses weighting factors based on collision kernels and leads to the result:

$$f(x) = \frac{(1-w)^{1-w}}{\Gamma(1-w)} x^{-w} \exp[-(1-w)x] \tag{6.63}$$

where Γ is the gamma function. For the constant-kernel case, where $w = 0$, eqn (6.63) reduces to the simple exponential form, as expected. For higher values of w, eqn (6.63) gives rather higher concentrations of large aggregates, but the overall form of the distribution is not greatly changed.

Since the simplest 'maximum entropy' method (Rosen, 1984) makes no assumptions about collision mechanisms or aggregate break-up, it is interesting to speculate on its applicability to aggregation in agitated systems. Here, orthokinetic collision processes and break-up of aggregates by shear also lead to a steady-state floc size distribution. In real systems it is not possible to analyse these processes in detail, but they are essentially stochastic in nature and a probabilistic approach might be fruitful.

Cohen (1991) has investigated steady-state size distributions in stirred suspensions, using an entropy approach and assuming that aggregation and break-up processes occur entirely at random. However, there is no way in which aggregate strength could be introduced into such a procedure. In the absence of detailed information, it seems reasonable to take the mean aggregate size as a variable to be determined empirically. By analogy with limiting floc sizes found in stirred suspensions, the mean size should depend on the stirring conditions and on the 'floc strength', which is affected by the nature of the particle interaction and hence by the additives used. Given an empirical value of the mean aggregate size, a 'scaling' relationship, perhaps the very simple exponential form of eqn (6.62), might then describe the aggregate size distribution reasonably well.

6.7 Flocculation by polymers

6.7.1 Introduction

In practical applications, suspensions are often flocculated by polymers and the mode of action of polymeric flocculants is broadly understood (Gregory, 1987). In many cases high molecular weight polymers are effective by virtue of a *bridging* mechanism, in which segments of a single polymer chain are adsorbed on more than one particle. With polyelectrolytes and oppositely charged particles, there is also the possibility of charge effects; either simple charge neutralization or some form of 'electrostatic patch' interaction (Gregory, 1976). In some texts the term 'flocculation' is used to imply aggregation by a polymer bridging mechanism, as distinct from 'coagulation' caused by the addition of salts and the consequent effect on double layer interaction (see Chapter 3). However, there are some difficulties in maintaining this distinction, e.g. in the case of polyelectrolytes, where the relative importance of polymer bridging and charge effects may not be known.

At the moment of addition of a polymer solution to a suspension of particles, usually under conditions of agitation, several processes are initiated, which are illustrated schematically in Figure 6.13:

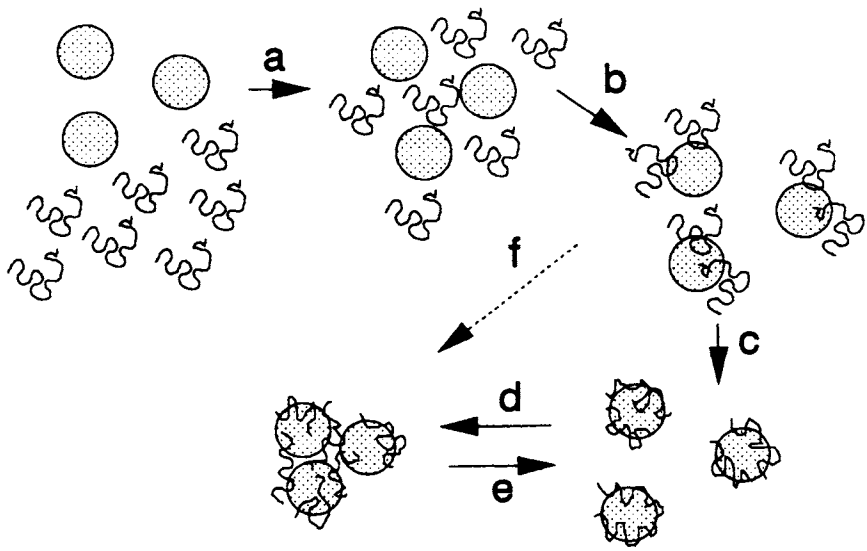

Figure 6.13 *Schematic illustration of the stages involved in the flocculation of a suspension by added polymer:* (a) *mixing of polymer chains among the particles;* (b) *adsorption of polymer;* (c) *re-conformation of adsorbed chains;* (d) *flocculation; and* (e) *break-up of flocs. The dashed arrow,* (f) *shows the possibility of bridging flocculation before the adsorbed chains have reached their equilibrium conformation*

(a) mixing of polymer solution throughout the suspension
(b) adsorption of polymer molecules on the particles, to give some degree of destabilization (either by charge neutralization or by giving opportunity for 'bridging' between particles)
(c) rearrangement of adsorbed polymer molecules from an initially extended state to a flatter, equilibrium conformation
(d) collisions between destabilized particles to give aggregates (flocs)
(e) break-up of flocs under the influence of applied shear.

These processes occur at different rates, which depend on a number of factors. Furthermore, they do not occur sequentially, but, to a large extent, concurrently, which makes the whole system difficult to analyse, but can help to explain the importance of mixing and dosing effects.

6.7.2 Mixing

In many cases, effective polymeric flocculants are of quite high molecular weight and are added as rather viscous solutions. For this reason the thorough distribution of polymer throughout the suspension may take some time and small droplets of polymer solution may persist for an appreciable fraction of the mixing time. These could possibly act as 'nuclei' for floc formation, although there is little evidence for such an effect (Stewart and Sutton, 1986). If the time needed for a thorough distribution of added polymer among the particles is long relative to the adsorption and flocculation rates, there may be significant practical consequences. For instance, excess polymer may adsorb on a fraction of the particles, which could then become restabilized. This effect is thought to be responsible for the residual haze and poor filterability found for some flocculated suspensions (Slater and Kitchener, 1966).

There is a good deal of evidence, largely empirical, that a high degree of turbulence at the point of addition of polymer solution can have a beneficial effect on the flocculation process. This is especially the case for fairly concentrated suspensions, where adsorption and particle collision rates are rapid. For instance, Warden (1984) found that the polymer-assisted thickening and dewatering of waterworks sludge could be greatly improved by careful attention to the polymer dosing point. It was shown that poor thickening was obtained at low and high values of applied shear, with intermediate values giving optimum results. There are many other applications, such as papermaking, where mixing conditions are known to be important.

Many laboratory flocculation trials are conducted in stirred vessels and the stirring rate can have a marked effect on the results. Such systems are complicated by the fact that there is a wide variation of effective shear rates (or energy dissipation) in a stirred vessel (Glasgow and Kim, 1986), so that floc formation and break-up may occur in different regions. It is typically found that flocs pass through a maximum size at some time after polymer dosing, and can show a marked reduction in size with continued stirring. These changes are reflected in dewatering rate (Kayode and Gregory, 1988) and settling rate (Li

Guibai and Gregory, 1991), which also reach maximum values after a certain stirring time.

By dosing polymer solution slowly or intermittently to a stirred suspension, considerable improvement in flocculation has been observed by Hogg (1989). In fact, Hogg showed that, in some cases, floc growth occurred only during polymer addition. Clearly, these effects must be closely related to mixing, since the more slowly polymer is added, the less likely is local overdosing and flocs are not allowed to grow very rapidly during the very early stages of the process.

6.7.3 Adsorption

It seems reasonable to suppose that the adsorption of polymer molecules on particles is a process that occurs at a transport-limited rate, at least in the early stages, when the fractional coverage is still quite low. In that case, the rate of adsorption depends on the rate of arrival of polymer molecules at a particle surface, and the number of encounters in unit time and unit volume can be written, by analogy with eqn (6.1):

$$J_{12} = k_{12} n_1 n_2 \tag{6.64}$$

where n_1 and n_2 are the number concentrations of particles and polymer molecules respectively and k_{12} is the appropriate rate constant (see below).

In practice, a certain fraction of added polymer needs to be adsorbed on particles to give adequate destabilization and hence allow flocculation to occur under the given shear conditions. If this fraction is f, then the time required for adsorption can be derived simply, assuming that the particle concentration remains constant, giving:

$$t_{\text{Ads}} = -\frac{\ln (1-f)}{k_{12} n_1} \tag{6.65}$$

A very important feature of this result is the inverse dependence on particle number concentration – the adsorption time will be lower at higher particle concentrations. The required time is also independent of the polymer concentration, provided that the same fraction of added polymer needs to be adsorbed. This last condition implies that the amount of adsorbed polymer needed to destabilize particles is proportional to particle concentration.

The adsorption rate constant can be estimated if it is assumed that both particles and polymer molecules can be treated as spheres. This assumption may seem unreasonable in the case of long-chain polymers, but such chains often adopt an approximately spherical, random coil conformation in solution and can be treated, hydrodynamically, as equivalent spheres. The transport of polymer molecules to particles may be by diffusion (perikinetic) or under the influence of fluid motion (orthokinetic). In each case, the rate constant can be derived from the appropriate Smoluchowski expression (see Gregory, 1988). For the perikinetic case, the rate constant is given by eqn (6.8) and the orthokinetic value is given by eqn (6.20).

The high shear forces present at a particle surface may reduce the adsorption rate and may even cause desorption of adsorbed polymer (Lee and Fuller, 1985). Although a quantitative analysis of this aspect is not yet possible, it may be one reason to expect an 'optimum' mixing intensity for flocculation by polymers.

Rate constants calculated from eqns (6.8) and (6.20) show that orthokinetic transport will often be much more significant than diffusion in promoting particle–polymer contacts (Gregory, 1988). This is the case for particles of about 1 μm in size or greater and polymer molecules larger than about 0.1 μm, with effective shear rates greater than about $50\,s^{-1}$ (see the numerical example in Section 6.7.5). Since typical polymer mixing conditions can correspond to shear rates of several hundred per second or greater, orthokinetic transport is likely to be important in most cases involving polymers of moderately high molecular weight. In such cases, the rate of polymer adsorption will depend strongly on the effective shear rate.

6.7.4 Reconformation

At equilibrium, an adsorbed polymer chain adopts a conformation consisting of trains, loops and tails, and a great deal of effort has been expended in both theoretical and experimental determinations of the segment density distribution as a function of distance from the adsorbing surface, (see, for example, Cosgrove, 1990). However, this equilibrium arrangement may be very different from the conformation of a polymer molecule in free solution and at the moment of initial contact with the particle.

The time over which the equilibrium conformation is attained can have a great influence on flocculation, since it is very likely that bridging contacts will occur more readily when the adsorbed polymer is in an extended, non-equilibrium state. When there is strong interaction between adsorbing polymer segments and the particle surface, e.g. between ionic groups of opposite sign, it is likely that a polymer chain will eventually lie flat on the surface, thus presenting no opportunity for bridging contacts. It could be argued that bridging contacts formed by polymer chains very soon after adsorption, or by simultaneous adsorption on two particles, would be weaker than those formed by adsorbed chains in a more 'flat' configuration. In the latter case, more segments of the chain would be attached to the particles and this should result in stronger binding between particles. Also, the more extended chains would occupy a smaller fraction of the particle surface and so the collision efficiency might be lower (see below).

Pelssers *et al.* (1990) assumed that adsorbed polymer chains would either be in an 'active' or 'inactive' state, the former corresponding to the extended, non-equilibrium condition in which bridging contacts are possible. After some time, relaxation to a flatter, inactive configuration occurs. The rate of this relaxation process depends on the nature of the polymer and on the particle–polymer interaction, but characteristic times of a few seconds for polymers with molecular weights of several million have been estimated (Cohen Stuart and Tamai, 1988). These times fit quite well the flocculation data of Pelssers *et al.* (1990). However,

very much longer relaxation times (many minutes or even hours) are indicated from experiments of Pefferkorn and Elaissari (1990), with quaternized polyvinyl pyridine of lower molecular weight (3.6×10^5).

At present, there is little other information which is of help in modelling the reconformation process under practical flocculation conditions. The effect of shear on the process seems to have been neglected.

6.7.5 Flocculation

The rate of aggregation (flocculation) depends on the collision rate of particles, also given by eqn (6.1). The value for the collision rate constant of primary particles, k_{11}, or the aggregation rate constant, $k_a (= k_{11}/2)$ can be used to calculate the characteristic aggregation time, τ, given by eqn (6.15).

It has been shown (Gregory, 1988) that this approach, applied to stirred suspensions and fairly high molecular weight polymers, predicts flocculation times considerably lower than adsorption times. A simple numerical example may be helpful.

Consider an aqueous suspension at 25°C, containing particles of 2 μm diameter at a number concentration of $10^{15}\,m^{-3}$. The suspension is stirred to give an effective shear rate of $50\,s^{-1}$, and 80% of the added polymer needs to be adsorbed to give effective destabilization. The polymer molecules are assumed to have an effective diameter of 200 nm (a reasonable value for a random coil polymer with a molecular weight of several million). It is then possible to calculate the appropriate rate constants from eqns (6.8) and (6.20) and then the times to give the required degree of adsorption from eqn (6.65). The characteristic aggregation times can be obtained from eqn (6.15). The following results are found:

	Perikinetic	*Orthokinetic*
t_{Ads}	43 s	7.8 s
τ	163 s	3.7 s

If the adsorption and aggregation are controlled only by diffusion (the perikinetic case), then the effective amount of polymer is adsorbed in a time which is appreciably less than the aggregation time. In this case the aggregation process would not be limited by the rate of adsorption. Under the assumed shear conditions, orthokinetic collisions increase the rates of both polymer adsorption and particle aggregation. However, the aggregation rate is more strongly influenced and the characteristic aggregation time becomes less than the adsorption time. In this case, the aggregation process would be limited by the relatively slow adsorption – particles would undergo several collisions before sufficient polymer had been adsorbed to give adequate destabilization.

Even when the added polymer is fully adsorbed, the collision efficiency may be less than unity, so that every collision does not result in permanent attachment. If the fraction of particle surface with adsorbed polymer is θ, and it is assumed that the only successful collisions are those between coated and uncoated surfaces, then it follows that the flocculation rate will depend on the product $\theta(1-\theta)$. This leads to the well-known 'half surface coverage' condition for optimum flocculation (Healy and La Mer, 1964). If the amount of polymer added to the suspension is not sufficient to give $\theta > 0.5$, then the collision efficiency should increase throughout the adsorption phase. It follows that there will be a period after polymer dosing during which particles are not yet sufficiently destabilized for flocculation to occur. For dilute suspensions this 'lag time' can be appreciable (several minutes). It can be reduced by increasing the shear rate, which increases both adsorption and flocculation rates. Such effects have been verified experimentally (Gregory and Lee, 1990).

For more concentrated suspensions, polymer adsorption is sufficiently rapid for flocculation to begin almost immediately after dosing. In such cases, mixing and reconformation effects can be very important.

6.7.6 Floc break-up

This topic has been considered briefly in Section 6.5. Although no adequate quantitative models are available, the break-up of flocs produced by polymers can be qualitatively very different from that of other aggregates. Long-chain polymers giving bridging flocculation lead to much stronger flocs (higher C values) than simple salts. Polyelectrolytes acting by charge neutralization give flocs of intermediate strength. Typically, flocs formed by polymer bridging can have diameters approaching 1 mm, which is larger than the microscale of turbulence (of the order of 100 μm in most cases).

A very important point concerning floc breakage is that it is often irreversible in the case of polymer bridging. Although flocs formed by long-chain polymers are more resistant to breakage, they tend not to re-form if breakage does occur. When charge neutralization is the mode of action, flocs are generally weaker, but can regrow after breakage if the shear rate is reduced (Ditter *et al*, 1982). Irreversible floc breakage has important implications for the choice of the duration and intensity of mixing during polymer dosing.

Bibliography

Chandrasekhar, S., Kac, M. and Smoluchowski, R. (1986) *Marian Smoluchowski. His Life and Scientific Work*, Polish Scientific Publishers, Warsaw

Dobiáš, B. (ed.) (1993) *Coagulation and Flocculation, Theory and Applications*, Marcel Dekker, New York

Sonntag, H. and Strenge, K. (1987) *Coagulation Kinetics and Structure Formation*, VEB Deutscher Verlag der Wissenschaften, Berlin

References

Adler, P. M. (1981) Heterocoagulation in shear flow. *J. Colloid Interface Sci.*, **83**, 106–115

Aubert, C. and Cannell, D. S. (1986) Restructuring of colloidal silica aggregates. *Phys. Rev. Lett.*, **56**, 738–741

Botet, R. and Jullien, R. (1984) Size distribution of clusters in irreversible kinetic aggregation. *J. Phys. A.*, **17**, 2517–2530

Brakalov, L. B. (1987) A connection between the orthokinetic coagulation capture efficiency of aggregates and their maximum size. *Chem. Eng. Sci.*, **42**, 2373–2383

Camp, T. R. (1953) Flocculation and flocculation basins. *Proc. ASCE*, **79**, 1–18

Camp, T. R. and Stein, P. C. (1943) Velocity gradients and internal work in fluid motion. *J. Boston Soc. Civ. Eng.*, **30**, 219–238

Cleasby, J. L. (1984) Is velocity gradient a valid flocculation parameter? *J. Env. Eng. ASCE.*, **110**, 875–897

Cohen R. D. (1991) Evolution of the cluster-size distribution in stirred suspensions. *J. Chem. Soc. Faraday Trans.*, **87**, 1163–1168

Cohen-Stuart, M. A. and Tamai, M. (1988) Dynamics of adsorbed polymers. I. Thickness relaxation of poly(vinyl pyrrolidone) on glass. *Macromolecules*, **21**, 1863–1866

Cosgrove, T. (1990) Volume fraction profiles of adsorbed polymers. *J. Chem. Soc. Faraday Trans.*, **86**, 1323–1332

Ditter, W., Eisenlauer, J. and Horn, D. (1982) Laser optical method for dynamic flocculation testing in flowing dispersions. In *The Effect of Polymers on Dispersion Properties*, (ed. Tadros, Th.F.) Academic Press, London, 323–342

Dukhin, S. S. and Lyklema, J. (1990) Dynamics of colloid particle interaction. Incomplete desorption relaxation. *Faraday Discuss. Chem. Soc.*, **90**, 261–269

Frens, G. and Heuts, J. J. F. G. (1988) The double layer potential ϕ_8 as a rate determining factor in the coagulation of electrocratic colloids. *Colloids Surfaces*, **30**, 295–305

Friedlander, S. K. (1977) *Smoke, Dust and Haze*, John Wiley, New York

Friedlander, S. K. and Wang, C. S. (1966) The self-preserving particle size distribution for coagulation by Brownian motion. *J. Colloid Interface Sci.*, **22**, 126–132

Fuchs, N. (1934) Über die Stabilität und Aufladung der Aerosole. *Z. Physik*, **89**, 736–743

Glasgow. L. A. and Kim, Y. H. (1986) Characterization of agitation intensity in flocculation processes. *J. Env. Eng. ASCE*, **112**, 1158–1163

Glasgow, L. A. and Liu, X. (1991) Response of aggregate structures to hydrodynamic stress. *AIChE J.*, **37**, 1411–1414

Gregory, J. (1976) The effect of cationic polymers on the colloidal stability of latex particles. *J. Colloid Interface Sci.*, **55**, 35–44

Gregory, J. (1987) Flocculation by polymers and polyelectrolytes. In: *Solid–Liquid Dispersions* (ed. Tadros, Th.F.) Academic Press, London, 163–181

Gregory, J. (1988) Polymer adsorption and flocculation in sheared suspensions. *Colloids Surfaces*, **31**, 231–253

Gregory, J. and Lee, S. Y. (1990) The effect of charge density and molecular mass of cationic polymers on flocculation kinetics in aqueous solution. *J. Water SRT-Aqua*, **39**, 265–274

Healy, T. W. and La Mer, V. K. (1964) Energetics of flocculation and redispersion by polymers. *J. Colloid Sci.*, **19**, 323–332

Higashitani, K., Miyafusa, S., Matsuda, T. and Matsuno, Y. (1980) Axial change of total particle concentration in Poiseuille flow. *J. Colloid Interface Sci.*, **77**, 21–28

Hoekstra, L. L., Vreeker, R. and Agterhof, W. G. M. (1992) Aggregation of nickel hydroxycarbonate studied by light scattering. *J. Colloid Interface Sci.*, **151**, 17–25

Hogg, R. (1989) The dynamics of polymer-induced flocculation of fine-particle suspensions. In *Flocculation and Dewatering*, (ed. Moudgil, B. M. and Scheiner, B. J.) Engineering Foundation,

New York, 143–151

Honig, E. P., Roebersen, G. J. and Wiersema, P. H. (1971) Effect of hydrodynamic interaction on the coagulation rate of hydrophobic colloids. *J. Colloid Interface Sci.*, **36**, 97–109

Jiang, Q. and Logan, B. E. (1991) Fractal dimensions of aggregates determined from steady-state size distributions. *Environ. Sci. Technol.*, **25**, 2031–2038

Kayode, T. O. and Gregory, J. (1988) A new technique for monitoring alum sludge conditioning. *Water Res.*, **22**, 85–90

Knocke, W. R. and Kelley, R. T. (1987) Improving heavy metal sludge dewatering characteristics by recycling preformed sludge solids. *J. Water Pollut. Control Fed.*, **59**, 86–91

Lagvankar, A. L. and Gemmell, R. S. (1968) A size–density relationship for flocs. *J. Am. Water Wks Assoc.*, **60**, 1040–1046

Lee, J-J and Fuller, G. G. (1985) Adsorption and desorption of flexible polymer chains in flowing systems. *J. Colloid Interface Sci.*, **103**, 569–577

Lee, K. W. (1983) Change of particle size distribution during Brownian coagulation. *J. Colloid Interface Sci.*, **92**, 315–325

Lee, K. W. (1985) Conservation of particle size distribution parameters during Brownian coagulation. *J. Colloid Interface Sci.*, **108**, 199–206

Li Guibai and Gregory, J. (1991) Flocculation and sedimentation of high-turbidity waters. *Water Res.*, **25**, 1137–1143

Lichtenbelt, J. W. Th., Pathmamanoharan, C. and Wiersema, P. H. (1974) Rapid coagulation of polystyrene latex in a stopped flow spectrophotometer. *J. Colloid Interface Sci.*, **49**, 281–285

Lin, M. Y., Lindsay, H. M., Weitz, D. A., Ball, R. C., Klein, R. and Meakin, P. (1989) Universality in colloid aggregation. *Nature*, **339**, 360–362

Meakin, P. (1988) Fractal aggregates. *Adv. Colloid Interface Sci.*, **28**, 249–331

Meesters, A. and Ernst, M. H. (1987) Numerical evaluation of self-preserving spectra in Smoluchowski coagulation theory. *J. Colloid Interface Sci.*, **119**, 576–587

Melik, D. H. and Fogler, H. S. (1984) Gravity-induced flocculation. *J. Colloid Interface Sci.*, **101**, 72–83

Michaels, A. S. and Bolger, J. C. (1962) The plastic flow behavior of flocculated colloidal sediments. *Ind. Eng. Chem. Fund.*, **1**, 153–162

Mühle, K. (1993) Floc stability in laminar and turbulent flow. In *Coagulation and Flocculation, Theory and Applications* (ed. Dobiáš, B.) Marcel Dekker, New York, 355–390

Mühle, K. and Domasch, K. (1991) Stability of particle aggregates in flocculation with polymers. *Chem. Eng. Process.*, **29**, 1–8

Ottewill, R. H. and Shaw, J. N. (1966) Stability of monodisperse polystyrene latex dispersions of various sizes. *Discuss. Faraday Soc.*, **42**, 154–163

Overbeek, J. Th. G. (1980) The rule of Schulze and Hardy. *Pure Appl. Chem.*, **52**, 1151–1161

Pefferkorn, E. and Elaissari, H. (1990) Adsorption–desorption processes in charged polymer/colloid systems; structural relaxation of adsorbed macromolecules. *J. Colloid Interface Sci.*, **138**, 187–194

Pelssers, E. G. M., Cohen Stuart, M. A. and Fleer, G. J. (1990) Kinetics of bridging flocculation. Role of relaxations in the polymer layer. *J. Chem. Soc. Faraday Trans.*, **86**, 1355–1361

Reerink, H. and Overbeek, J. Th. G. (1954) The rate of coagulation as a measure of the stability of silver iodide sols. *Discuss. Faraday Soc.*, **18**, 74–84

Rosen, J. M. (1984) A statistical description of coagulation. *J. Colloid Interface Sci.*, **99**, 9–19

Saffman, P. G. and Turner, J. S. (1956). On the collision of drops in turbulent clouds. *J. Fluid Mech.*, **1**, 16–30

Slater, R. W. and Kitchener, J. A. (1966) Characteristics of flocculation of mineral suspensions by polymers. *Discuss. Faraday Soc.*, **42**, 267–275

Smoluchowski, M. (1917) Versuch einer mathematischen Theorie der Koagulationskinetic kolloider Lösungen. *Z. Phys. Chem.*, **92**, 129–168

Sonntag, H. (1993) Coagulation kinetics. In *Coagulation and Flocculation, Theory and Applications* (ed. Dobiáš, B.) Marcel Dekker, New York, 57–99

Spielman, L. A. (1970) Viscous interactions in Brownian coagulation. *J. Colloid Interface Sci.*, **33**, 562–571

Spielman, L. A. (1978) Hydrodynamic aspects of flocculation. In *The Scientific Basis of Flocculation* (ed. Ives, K. J.) Sijthoff and Noordhoff, Alphen aan den Rijn, 63–88

Stewart, R. F. and Sutton, D. (1986) Characterization of the structure of concentrated flocculated suspensions. *Part. Sci. Technol.*, **4**, 251–264

Swift, D. L. and Friedlander, S. K. (1964) The coagulation of hydrosols by Brownian motion and laminar shear flow. *J. Colloid Sci.*, **19**, 621–647

Tambo, N. and François, R. J. (1991) Mixing, breakup and floc characteristics. In *Mixing in Coagulation and Flocculation.* (ed. Amirtharajah, A., Clark, M. M. and Trussell, R. R.) American Water Works Association Research Foundation, Denver, 256–281

Tambo, N. and Watanabe, Y. (1979) Physical aspects of flocculation. I. The floc density function and aluminium floc. *Water Res.*, **13**, 409–419

Tence, M., Chevalier, J. P. and Jullien, R. (1986) On the measurement of the fractal dimension of aggregated particles by electron microscopy: experimental method, corrections and comparison with numerical models. *J. Phys.*, **47**, 1989–1998

Torres, F. E., Russel, W. B. and Schowalter, W. R. (1991a) Floc structure and growth kinetics for rapid shear coagulation of polystyrene colloids. *J. Colloid Interface Sci.*, **142**, 554–574

Torres, F. E., Russel, W. B. and Schowalter, W. R. (1991b) Simulations of coagulation in viscous flows. *J. Colloid Interface Sci.*, **145**, 51–73

van de Ven, T. G. M. and Mason, S. G. (1977) The microrheology of colloidal suspensions. VII. Orthokinetic doublet formation of spheres. *Colloid Polymer Sci.*, **255**, 468–479

van de Ven, T. G. M. and Mason, S. G. (1981) Comparison of hydrodynamic and colloid forces in paper machine headboxes. *Tappi*, **64**, 171–175

Vold. M. J. (1963) Computer simulation of floc formation in a colloidal sediment. *J. Colloid Sci.*, **18**, 684–695

Warden, J. H. (1984) Thickening and dewatering of hydroxide sludges. In *Solid–Liquid Separation* (ed. Gregory, J.) Ellis Horwood, Chichester, 89–99

Warren, L. J. (1981) Shear flocculation. *Chemtech*, **11**, 180–185

Wiesner, M. R. (1992) Kinetics of aggregate formation in rapid mix. *Water Res.*, **26**, 379–387

Zollars, R. I. and Ali, S. I. (1986) Shear coagulation in the presence of repulsive interparticle forces. *J. Colloid Interface Sci.*, **114**, 149–166